Changes in optical characteristics of surface microlayers hint to photochemically and microbially-mediated DOM turnover in the upwelling region off the coast off Peru

Luisa Galgani[1,2], and Anja Engel[1*]

[1] GEOMAR – Helmholtz Centre for Ocean Research Kiel, Düsternbrooker Weg 20, 24105 Kiel, Germany

[2] Alfred-Wegener-Institute – Helmholtz Centre for Polar and Marine Research, Am Handelshafen 12, 27570 Bremerhaven, Germany

* aengel@geomar.de, tel. +494316001510

Abstract

The coastal upwelling system off Peru is characterized by high biological activity and a pronounced subsurface oxygen minimum zone, as well as associated emissions of atmospheric trace gases such as N_2O, CH_4 and CO_2. During the METEOR (M91) cruise to the Peruvian upwelling system in 2012, we investigated the composition of the sea-surface microlayer (SML), the oceanic uppermost boundary directly subject to high solar radiation, often enriched in specific organic compounds of biological origin like Chromophoric Dissolved Organic Matter (CDOM) and marine gels. In the SML, the continuous photochemical and microbial recycling of organic matter may strongly influence gas exchange between marine systems and the atmosphere. We analyzed SML and underlying water samples at 38 stations focusing on CDOM spectral characteristics as indicator of photochemical and microbial alteration processes. CDOM composition was characterized by spectral slope (*S*) values and Excitation-Emission Matrix fluorescence (EEMs), which allow to track changes in molecular weight (MW) of DOM, and to determine potential DOM sources and sinks. We identified five fluorescent components (F1-5) of the CDOM pool, of which two had excitation/emission characteristics of amino-acid like fluorophores (F1, F4) and were highly enriched in the SML. CDOM composition and changes in spectral slope properties suggested a local microbial release of DOM directly in the SML as a response to light exposure in this extreme environment. In a conceptual model of the sources and modifications of optically active DOM in the SML and underlying seawater (ULW), we describe processes we think may take place (see graphical abstract): The production of CDOM of higher MW by microbial release through growth, exudation and lysis in the euphotic zone, includes the identified fluorophores (F1, F2, F3, F4, F5). Specific amino-acid like fluorophores (F1, F4) accumulate in the SML with respect to the ULW, as photochemistry may enhance microbial CDOM release by a) photoprotection mechanisms and b) cell-lysis processes. Microbial and photochemical degradation are potential sinks of the amino-acid like fluorophores (F1, F4), and potential sources of reworked and more refractory humic-like

components (F2, F3, F5). In the highly productive upwelling region along the Peruvian coast, the interplay of microbial and photochemical processes controls the enrichment of amino-acid like CDOM in the SML. We discuss potential implications for air-sea gas exchange in this area.

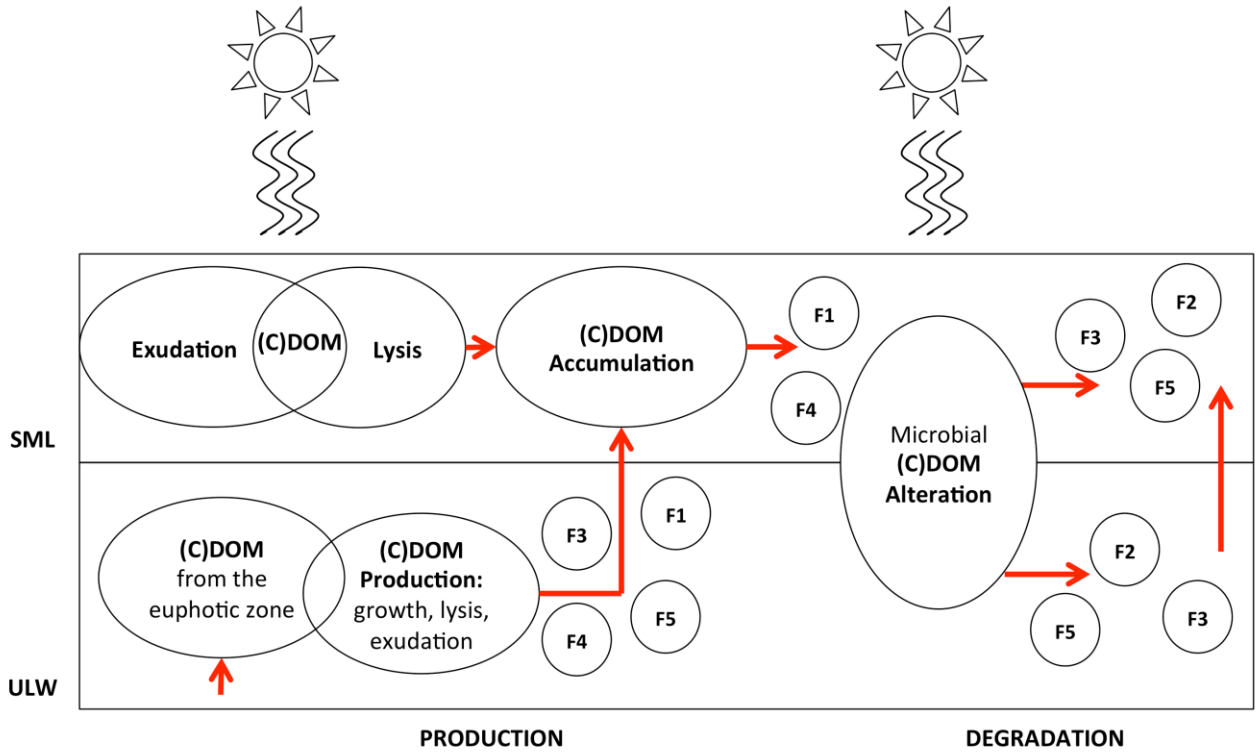

1. Introduction

The Peruvian Eastern Boundary Upwelling System (EBUS), extending along the coast off Peru between 4° and about 40° South, is among the most productive marine ecosystems worldwide (Capone and Hutchins, 2013;Chavez and Messié, 2009;Rosenberg et al., 1983) and it is characterized by high biological activity, involving high export rates of organic carbon both vertically and laterally (Arístegui et al., 2004;Muller-Karger et al., 2005). The high productivity is sustained by winds year-round that promote the upwelling of nutrient-rich deep waters into the euphotic zone, thus favoring phytoplankton photosynthesis and organic matter production (Chavez and Messié, 2009). High rates of organic matter production are counterbalanced by heterotrophic respiration, which provides sinks for the oxygen produced by autotrophs and leads to subsurface

Oxygen Minimum Zones (OMZs) (Lachkar and Gruber, 2011). OMZs are expanding worldwide due to reduced solubility at increasing temperatures, as well as a consequence of reduced oceanic ventilation and enhanced stratification (Keeling et al., 2010;Stramma et al., 2008). OMZ become increasingly important as key marine regions for the emission of climate-relevant gases like carbon dioxide (CO_2), methane (CH_4), nitrous oxide (N_2O) and hydrogen sulfide (H_2S) (Paulmier et al., 2008;Paulmier et al., 2011). N_2O is a strong greenhouse gas and ozone-reactive: 30% of its atmospheric concentration has an oceanic source (Solomon et al., 2007), of which, up to 75% is supported by OMZs (Bange et al., 2001). Therefore, OMZs are key environments to assess the oceanic contribution to the concentration of atmospheric gases. Defining the processes that regulate gas fluxes across the water-air interface is a central objective to better understand the reciprocal relationship between changes in our climate and marine environments.

The uppermost oceanic layer in contact with the atmosphere is the sea-surface microlayer (SML), which mediates major climate-relevant processes including air-sea gas exchange and sea-spray aerosol emission (Liss and Duce, 2005). This interface between a liquid (hydrosphere) and a gas phase (atmosphere) accumulates organic matter of biological origin, creating a sort of "skin" of surface-active compounds able to damp capillary waves and "capping the flux" of gases across the water-air interface (GESAMP, 1995). Natural organic compounds in the SML include a vast array of photosynthesis products including carbohydrates, amino acids and lipids, as well as other carbon-rich compounds like dissolved organic matter (DOM) and marine gels (e.g. Cunliffe et al., 2013). The DOM pool represents a continuum of molecular weights and biological lability ranging from refractory to labile DOM being utilized rapidly by microorganisms (Benner, 2002;Carlson, 2002), or photochemically degraded (Kieber, 2000). These compounds, produced in the oceanic photic zone and brought to the SML through rising bubbles (Hardy, 1982), contribute to the enrichment of a natural surface biofilm and favor specific SML heterotrophic communities that are very active in recycling this organic material (Hardy, 1982;Cunliffe et al., 2011). While bulk dissolved organic carbon is not generally enriched in the SML, specific DOM fractions are present occasionally at

much higher concentrations than in the underlying water (Cunliffe et al., 2013). These enriched pools of organic matter include marine gel particles (Wurl and Holmes, 2008), chromophoric dissolved organic matter (CDOM) (Zhang and Yang, 2013;Tilstone et al., 2010) and phenolic material (Carlson, 1982;Carlson and Mayer, 1980).

CDOM is the principal light-absorbing constituent of DOM, strongly absorbing UV (100 - 400 nm) and visible radiation (400 - 700 nm), and it can comprise 20%-70% of the DOM in oceanic waters (Coble, 2007). CDOM plays a major role in the attenuation of UV wavelengths and can reduce the availability of underwater photosynthetically active radiation for primary production (Bracchini et al., 2011). Photolysis of CDOM promotes the formation of low molecular weight (LMW) compounds from the breakdown of high molecular weight DOM (HMW-DOM), facilitating the bioavailability of carbon uptake for microbial growth from biologically refractory material, and representing an important loss pathway for CDOM in the oceans (Kieber et al., 1989). Other major by-products of CDOM photolysis are carbon monoxide (CO), which often exists at supersaturated concentrations in the oceans' surface (Blough, 2005, and references therein), CO_2 (Miller and Zepp, 1995) and reactive chemical species (Loiselle et al., 2012). To initiate a photochemical reaction, light must first be absorbed and in this respect the SML is very well exposed to elevated solar radiation (Liss and Duce, 2005). CDOM photolysis may affect biological processes within the SML as well as the structure of accumulated organic matter. Optical properties and photochemical cycling of DOM have been widely investigated in the ocean: CDOM alters light spectra in the surface ocean and its spatial and temporal distribution have been used in characterizing water masses exchange (Nelson and Siegel, 2013). However, processes within the SML remain poorly understood. Possible effects of photochemistry on SML chemical composition have been discussed in the past (Blough, 2005), but still little is known on CDOM fluorophores, sources and sinks (Tilstone et al., 2010;Zhang and Yang, 2013). To discern sources, sinks and modification of DOM in surface waters, whether microbially or photochemically-induced, we investigated optical properties of organic sea-surface microlayers and underlying water samples in the highly productive

EBUS off Peru. We applied optical spectroscopy measurements combined with chemical and biological analysis to identify different compounds within the CDOM pool and their partitioning between the SML and the underlying water. The use of excitation-emission matrix fluorescence spectroscopy (EEMs) allowed us to discriminate different compound classes in the SML and underlying water based on their excitation and emission maxima (Coble, 1996).

At present, the oceans are subject to many changes in physical and chemical properties like pH, temperature, and dissolved oxygen concentration, which potentially will affect the biological cycling of carbon (Riebesell et al., 2009;Keeling et al., 2010;Bopp et al., 2002). Whether the oceans are sources or sinks of carbon depends on the production rate of organic matter with respect to its biological degradation (Del Giorgio and Duarte, 2002), and high DOM degradation in the SML might represent a net source of CO_2 to the atmosphere (Garabétian, 1990). It is well known that the composition of the SML reflects biological processes of the euphotic zone (Galgani et al., 2014;Gao et al., 2012;Matrai et al., 2008;Bigg et al., 2004), and that elevated concentrations of organic matter may accumulate in the SML in highly productive regions like the Peruvian EBUS (Engel and Galgani, 2016). The enrichment of light-absorbing DOM in the SML may increase the photochemical formation and fluxes of reactive chemical species at the surface, with potentially important consequences for the composition of the SML itself and for the fate of compounds passing through this interface (Blough, 2005). Last but not least, the photochemical DOM breakdown may increase the biological availability of carbon, thus increasing heterotrophic respiration and CO_2 flux to the atmosphere.

CDOM contributes to the dissolved organic carbon (DOC) pool, but while DOC is a bulk measure, CDOM is a characteristic of DOM rather than a discrete class of compounds (Nelson and Siegel, 2013). Positive correlations have been observed between CDOM and DOC in coastal systems and plankton enclosures (Loginova et al., 2015), but the strenght of these correlations varies much across regional and seasonal differences (Blough and Del Vecchio, 2002). CDOM is a precursor for photochemical reactions that may drive the emission of trace gases from photochemically-altered

DOM (e.g. Ciuraru et al., 2015). Therefore, in upwelling areas associated with OMZs, CDOM characteristics in the SML are worth to be investigated as they may impact the exchange of gases between the ocean and the atmosphere.

2. Material and methods

2.1. Study area

The R/V METEOR cruise M91 was an integrated biogeochemical study in the upwelling region off Peru, with the aim to assess the importance of oxygen minimum zones (OMZs) for the air-sea exchange of gases relevant for climate and tropospheric chemistry (Bange 2013). A total of 39 samples for SML and underlying water were collected in December 2012 between 5°S and 16°S off the Peruvian coast. Data that we report here additionally from what previously described by Engel and Galgani (2016) refer to 38 stations. For easiness of comparison, table 1 recalls salinity, water temperature, radiation and wind speed, as already described in the companion manuscript (Engel and Galgani, 2016).

Some stations were revisited for multiple sampling (Table 2): S7 and S7_2; S12_1, S12_2, and S12_3; S16_1, S16_2, S16_3; S20 and S20_2. These stations were sampled within a time frame of 24 hours for SML and ULW, as we were interested in monitoring the evolution of CDOM optical properties in the SML and ULW at different times of the day depending on the solar irradiation. Whenever possible, we sampled at sunrise, midday and sunset. For security reasons, it was not possible to sample later than sunset, as the zodiac operations were not allowed out at dark. Exact latitude and longitude were not always possible to retrieve after a certain time, but were similar for the stations sampled in a few hours time lag.

The sampling approach for the SML was chosen as a silicate glass plate of 500 mm (length) x 250 mm (width) x 5 mm (thickness) with an effective sampling area of 2000 cm^2 as indicated in Engel and Galgani (2016). Briefly, the glass plate was inserted into the water perpendicular to the surface and withdrawn at a controlled rate of ~ 20 cm s^{-1} as first suggested by Harvey and Burzell (1972).

Different devices can be applied to sample the SML. The glass plate approach we choose collects a thinner SML (~60 - 150 µm) when compared to i.e. the Garrett Screen (150 - 300 µm), one of the mainly recognized practices introduced by Garrett in 1965 (Cunliffe et al., 2011; Garrett, 1965). The glass plate was chosen because it allows the sampling of enough volume required for analysis while keeping a minimal dilution with underlying water. Sampling was performed on a rubber boat; in order to obtain a well-standardized procedure and to minimize biases by sampling, the same person always took the samples with a repeatable withdrawal speed of the SML. The rubber boat was positioned as far upwind of the ship as possible and away from the path taken by the ship in order to avoid any potential surface contamination. The outboard motor of the rubber boat was switched off and samples were collected in upwind clean waters.

Before collecting the sample into the bottle, we let the plate drain for 20 s approximately. Then, the sample retained on both sides of the plate was removed with a Teflon wiper, and the procedure repeated about 20 times to obtain the necessary volume for analysis. The exact amount of dips per sample has been tracked. The first sample was discarded and used to rinse the collecting bottle (HCl 10% cleaned and Milli-Q rinsed). Glass plate and wiper were acid cleaned (HCl 10%) and Milli-Q rinsed prior use, and at sampling site they were copiously rinsed with in situ seawater to minimize any contamination with alien material during transport and handling. Underlying seawater (ULW) was collected right after SML at about ~ 20 cm depth by opening an acid cleaned (HCl 10%) and Milli-Q rinsed glass bottle and closing it underwater. The thickness (*d, m*) of our reference SML that we were able to collect was estimated as follows:

(1) $d = V/(A \times n)$

Where V is the SML volume collected, i.e. 60-140 mL, A is the sampling area of the glass plate (A = 2000 cm²) and n is the number of dips. During this cruise, the apparent sampling thickness of the SML ranged between 45 and 60 µm, with an overall mean of 49 ± 8.9 µm (Engel and Galgani, 2016). Many factors may influence the thickness of the SML such as withdrawal rate, dipping time, and plate dimensions. With a withdrawal speed of ~ 20 cm s^{-1}, the apparent SML thickness was in

accordance with previous findings at similar withdrawal rate reporting 60 – 100 µm (Harvey and Burzell, 1972) and 50 – 60 µm (Zhang et al., 1998). The sampling thickness was very well comparable among all stations, indicating that no major biases due to sampling procedure may have occurred.

After sampling, bottles were stored in the dark and the samples immediately processes in the laboratory onboard, within maximum 30 minutes from sampling.

2.2. Chemical and biological analyses

Dissolved organic matter (DOM): Sampling, calibration and analysis procedure for dissolved organic carbon (DOC) and for dissolved hydrolysable amino acids (DHAA), have been described in details in Engel and Galgani (2016). Additionally, to track DOM diagenetic state and bioavailability, we used the carbon-normalized yields of dissolved amino acids to DOC, expressed as DHAA%-DOC (Amon and Fitznar, 2001;Benner, 2002;Kaiser and Benner, 2009;Davis and Benner, 2007). Amino acids generally comprise a large fraction of bioavailable organic matter and are preferentially consumed by microbial activity quite rapidly. In surface waters they may be easily photodegraded too. Therefore, the amount of carbon included in amino acids is considered as a good indicator of DOM diagenesis and a value of ~ 2% of DHAA%-DOC may indicate the threshold between labile and semi-labile and refractory DOM (Davis and Benner, 2007).

Samples for chromophoric and fluorescent DOM (CDOM and FDOM) were filtered through 0.45 µm PES syringe filters and collected into 40 mL pre-combusted (8 h, 500° C) amber glass vials. Samples were stored in the dark at 4° C with no other treatment than pre-filtering. Since storage procedures may affect the absorbance and fluorescence properties of DOM, absorbance and fluorescence readings were performed directly on-board within a few hours from sampling or the next day according to Schneider-Zapp and colleagues (2013). Prior to measurements, samples were stored in the dark and acclimatized at room temperature. For CDOM, triplicate absorbance measurements were made on a Shimadzu 1800 UV-Visible Spectrophotometer in the range 220 to

700 nm with 0.5 nm increments, in a 10 cm path-length quartz cuvette against Milli-Q water as a reference. For FDOM, 3-D fluorescence spectroscopy was performed with a Varian Cary Eclipse Fluorescence Spectrophotometer equipped with a xenon flash lamp and data assembled into Excitation/Emission matrices (EEMs) which enable to individuate single DOM fluorophores (Coble, 1996) and to perform parallel factor analysis PARAFAC (Stedmon and Bro, 2008). Samples have been acclimatized and scanned at a fixed 20°C temperature (Cary Single Cell Peltier Accessory, VARIAN) in 1 cm path length quartz cuvette. Scans were performed at 600 nm/min using an excitation range (Ex) of 240-450 nm with 5 nm increments and recorded emission (Em) in the range 242-600 nm with 2 nm increments. Samples were run in a mode of 5 nm slit for both excitation and emission and 0.1 s integration time.

Particulate Organic Carbon (POC) and gel particles: Total numbers of gel particles were determined by microscopy after Engel (2009). A detailed description of the method used during M91 cruise can be found in Engel and Galgani (2016). POC data were retrieved after Engel and Galgani (2016). We refer to this companion publication for further analytical details.

Phytoplankton and heterotrophic bacteria: Samples, calibration and analysis for phytoplankton and heterotrophic bacteria counts for M91 are described in details in Engel and Galgani (2016).

2.3. Data analysis

CDOM: The measured absorbance at every wavelength λ was converted to absorption coefficient $a(\lambda)$, (m^{-1}), according to the following equation (Bricaud et al., 1981):

$$(2)\quad a(\lambda) = 2.303A_{\lambda}/L$$

where A_{λ} is the absorbance and L is the path-length of the cuvette (here 0.10 m). Absorbance is an optical characteristic of CDOM, which allows quantifying the amount of CDOM in the samples. Therefore, the absorption coefficient $a(\lambda)$ is considered as a proxy for CDOM concentration. To estimate CDOM concentration, we calculated the absorption coefficient at 325 nm as often used for the open ocean (Swan et al., 2009;Nelson and Siegel, 2013). The dependence of a on the

wavelength was determined by analyzing the spectral slope parameter S (nm^{-1}) in the discrete wavelength ranges of 275-295 nm and 350-400 nm, determined by linear regression of log-transformed absorption spectra against the wavelength (Bricaud et al., 1981;Helms et al., 2008):

(3) $a(\lambda) = a(\lambda_0)e^{-S(\lambda - \lambda_0)}$

where $a(\lambda_0)$ is the absorption coefficient at a reference wavelength λ_0. S measured in the wavelength range 275-295 nm (S(275-295), nm^{-1}) and 350-400 nm (S(350-400), nm^{-1}) as well as slope ratio (SR) defined as S(275-295): S(350-400) are good indicators to characterize CDOM (Helms et al., 2008). SR is characterized by lower values for terrestrial CDOM compared to CDOM produced by autochthonous marine sources and instead of S alone, could be a more sensitive indicator of photochemically induced changes in the molecular weight of the CDOM pool as an increase in SR suggests photodegradation processes, while a decrease is often related to microbially altered CDOM (Helms et al., 2008). Both S(275-295) and SR increase with a) irradiation (photobleaching), b) with decreasing DOM molecular weight, and c) at higher salinity reflecting mixing of water masses along a salinity gradient. As such they are useful as tracers to determine mixing and coastal inputs. We also determined the $SUVA_{254}$ index, that is, the specific ultraviolet absorbance (A) at 254 nm normalized to DOC concentration. This index was shown to correlate significantly with increasing aromaticity of DOM (Weishaar et al., 2003):

(4) $SUVA_{254}$ (mg C L^{-1} m^{-1}) = A(254) (m^{-1})/ DOC (mg L^{-1})

FDOM: The 3-D recorded spectra were corrected for the instrumental biases both for excitation and emission using correction curves provided by the manufacturer (Stedmon and Bro, 2008). Additionally, spectra were corrected against a Milli-Q water blank run every day before the samples to remove water Raman peaks. No correction for inner filter effects was applied to our data as for each sample the relative $a(\lambda)$ value was below 10 m^{-1} (Lawaetz and Stedmon, 2009;Stedmon and Bro, 2008). As an example, a(254) was on average 2±2 m^{-1} for SML and 1.6±1.3 m^{-1} for underlying water (ULW) samples. Fluorescence spectra were normalized to Raman Units (R.U.) by integrating the Raman peak of 350 nm Ex and 382 to 407 nm Ex extracted by the daily Milli-Q water blank.

271 Calibration to R.U. was done with the FDOMcorrect toolbox for Matlab (The MathWorks Inc.)
272 incorporated in DrEEM toolbox (Murphy et al., 2013). We choose to normalize to R.U. as these
273 units are widely used in open ocean measurements and we could compare our results.
274 PARAFAC analysis was applied to EEMs in order to identify and quantify independent underlying
275 components of the CDOM pool, and was performed by the N-way toolbox for Matlab in DrEEM
276 (Murphy et al., 2013). After normalization to R.U. units, data were smoothed to remove remaining
277 scatter peaks, Raman and Rayleigh signals by creating a sub-dataset. We then performed a
278 preliminary outlier analysis generating models with 3 to 7 factors with non-negativity constraints,
279 comparing the spectra to unconstrained models. When dilution dominates the dataset, components
280 are strongly correlated. To investigate biases due to dilution, we performed a test for correlations
281 between the components, as suggested by the DrEEM tutorial by Murphy and colleagues (2013).
282 We then normalised the dataset by the DrEEm function *normeem* to reduce the co-linearity related
283 to the concentration, thus giving low-concentrated samples a possibility to enter the model,
284 followed by the outlier test again on the normalised data. After visually comparing the spectra and
285 looking at the error residuals for models with 4 to 7 components, we then compared the models by
286 the sum of squared errors (SSE) expressed as a function of wavelength, choosing the models with
287 lower SSE. At this stage, we choose models with 5, 6 and 7 components and reversed the
288 normalization to obtain the unscaled scores before validation. Models with 5, 6 and 7 components
289 were validated by split half analysis "$S_4C_6T_3$" (see Murphy et al. 2013) where it was ensured that in
290 each test the dataset halves being compared had no samples in common. The validation was
291 successful for 5-components model, for all comparison. The maximum fluorescence intensities of
292 the five fluorophores at specific Ex-Em wavelengths ranges are described in table 3. Figures with
293 the model comparison for both excitation and emission for the 5-components model are included in
294 the supplementary material (Figures S1 and S2).
295 In fluorescence spectroscopy, the humification index (HIX), first introduced by Zsolnay et al.
296 (1999), is a powerful tool to study CDOM dynamics in soils, as humification is associated with a

297 shift to longer emission wavelengths (Senesi, 1990). It has been first applied to aquatic CDOM in
298 estuarine waters by Huguet and colleagues (2009), and is calculated as the ratio H/L of two spectral
299 region areas of the emission spectrum scanned at 254 nm excitation. Area L is calculated between
300 the emission wavelengths 300 nm and 345 nm, and area H between 435 nm and 480 nm. When the
301 degree of aromaticity of CDOM increases, the emission spectrum at excitation 254 nm is shifted
302 towards the red (longer wavelengths), implying an increase in H/L ratio and in HIX. High HIX
303 implies maximum fluorescence intensity at long wavelengths and therefore the presence of complex
304 molecules like HMW aromatic CDOM (Senesi et al., 1991). We applied a slight modification to the
305 HIX index for our samples, introducing the "SMHIX" index, where SM stands for Surface
306 Microlayer. As we did neither have the scanned excitation wavelength of 254 nm, nor the scanned
307 spectrum at excitation 345 nm and 435 nm, we calculated SMHIX index as follows:

308 (5) $\mathrm{SMHIX} = (\sum \mathrm{I}_{434\rightarrow480}) / \sum \mathrm{I}_{300\rightarrow346}$

309 Where $\sum I_{434\rightarrow480}$ is the sum of all fluorescence intensities at every emission wavelength between
310 434 nm and 480 nm, and $\sum I_{300\rightarrow346}$ is the sum of all fluorescence intensities at every emission
311 wavelength between 300 nm and 346 nm, both scanned with excitation = 255 nm.

312 **Enrichment Factors:** Enrichment Factors (EF), allow tracking of accumulation patterns of any
313 compound in the SML with respect to the underlying water (ULW) and comparison among
314 different compounds. EF are calculated according to the following:

315 (6) $\mathrm{EF} = [\mathrm{X}]_{\mathrm{SML}} / [\mathrm{X}]_{\mathrm{ULW}}$

316 Where [X] is the concentration of a given parameter in the SML or ULW, respectively (GESAMP,
317 1995). EF > 1 indicates an enrichment, EF < 1 indicates a depletion in the SML. EFs are normally
318 used for quantitative parameters, i.e., measured in abundance and concentration such as DOC,
319 DHAA, CDOM, marine gels and cell abundances. Here, we applied the EF calculation for
320 qualitative ratios and indexes too, like *S*(275-295), SR, SMHIX, SUVA_{254}, DHAA%-DOC. We
321 kept the same wording, which is useful to describe differences between SML and ULW for both
322 quantitative and qualitative parameters.

Statistical tests in data analysis have been accepted as significant for $p < 0.05$. Calculations, statistical tests and illustration were performed with Microsoft Office Excel 2010, Sigma Plot 12.0 (Systat), Prism (GraphPad), Ocean Data View and Matlab R2009b (The MathWorks Inc.).

3. Results

Results on dissolved organic carbon and amino acids, gel particles (TEP and CSP), phytoplankton and bacterial abundance and the relative enrichment of these components in the SML of our sampling sites have been described elsewhere (Engel and Galgani, 2016). Here, we focus on the optical properties of DOM to identify possible sources, sinks and dynamics in the SML and underlying water of the Peruvian upwelling region.

3.1. CDOM optical absorption properties

In the upwelling region off Peru, values for CDOM absorption coefficient $a(325)$ ranged from 0.09 to 1.47 m^{-1} in the SML and from 0.07 to 1.47 m^{-1} in ULW. Highest values were observed at stations S10_1 to S10_4 along the coast for both SML and ULW. CDOM was enriched in the SML at most stations (Figure 3), with median EF for $a(325) = 1.2$ in a range varying between 0.4 and 2.8. A median EF = 1.2 means that at least 50% of our observations accounted for a CDOM-enriched SML. Besides the southern transect, higher EF values were observed at the northern stations S2 and S2_2, and in the southern coastal upwelling stations S15_1 to S15_3. Lower EFs and EFs < 1, indicating a depletion of CDOM in the SML, were observed at higher distance from the coast (Figure 4).

The spectral slope parameter between 275 and 295 nm ($S(275\text{-}295)$, nm^{-1}) is a good indicator for CDOM molecular weight as an increase of this parameter indicates decreasing molecular weight, thus revealing accumulation or degradation processes of bioavailable CDOM (Helms et al., 2008). In our samples, $S(275\text{-}295)$ ranged from 0.012 to 0.038 nm^{-1} in the SML and from 0.017 to 0.043 nm^{-1} in ULW. In general, $S(275\text{-}295)$ was quite similar between SML and ULW, and no statistically

significant differences were found between SML and ULW for *S*(275-295). Higher spectral slopes were observed in the ULW of the southern stations below 15°S (S19, S19_2, S20, S20_2, S1778). In the coastal stations S10_1 to S10_4 and S14_1 to S15_3 lower *S*(275-295) values were determined for both SML and ULW. Median enrichment factor (EF) for *S*(275-295) was 1 (Figure 3), thus indicating similar molecular weight of CDOM compounds in the SML and ULW. Lower EFs were observed in the northernmost and southernmost stations and along the coast.

The $SUVA_{254}$ and SMHIX indexes are related to the degree of CDOM aromaticity and to its humic content, respectively. In our study, SUVA254 ranged from 0.49 to 1.74 mg C L^{-1} m^{-1} in the SML, with highest values at coastal southern stations S10_1 to S10_4 and S14_1 to S17_2. Similar values were recorded for ULW, ranging from 0.49 to 1.21 mg C L^{-1} m^{-1}. Generally, $SUVA_{254}$ values in our samples were comparable to the Pacific Ocean with a typical $SUVA_{254}$ of 0.6 mg C L^{-1} m^{-1} (Helms et al., 2008;Weishaar et al., 2003). Median EF for $SUVA_{254}$ was 1.1, with higher values in correspondence of northern stations and coastal southern stations (S2, S2_2, S15_1 to S15_3 and S19 to S1778) where the higher EF for *a*(325) were also observed (Figures 3 and 4). SMHIX ranged from -1.33 to 2.05 for SML and from -0.1 to 3.03 for ULW, with highest values in ULW. Enrichment factors showed an overall depletion of high-humic acid containing CDOM in the SML (Figure 3), with median EF = 0.8. Higher humic acid enrichment in the SML was observed on the southern transect S19 to S1778 (Figure 4), where we recorded the highest enrichment of CDOM (as *a*(325)) as well.

The carbon-normalized yields of dissolved amino acids (DHAA%-DOC) as indicator of DOM diagenetic state, ranged from 1.4% to 8.1% in SML samples and from 0.9% to 3.6% in ULW samples, indicating relatively more labile DOM in the SML. This observation was supported by the enrichment factors (EF), which showed a general enrichment of more labile DOM in the SML (Figure 3), with median EF values for DHAA%-DOC of 1.5. Highest EFs were recorded in the northernmost stations S1 to S3, and on the southernmost transect S19 to S1778.

3.2. PARAFAC analysis for CDOM fluorophores

Five optically active components were identified by PARAFAC analysis with the DrEEM toolbox in Matlab (Murphy et al., 2013), hereafter named F1, F2, F3, F4 and F5 (Figure 5). The spectral characteristics of the five identified components were compared to previous studies as described in table 3. F1 had an excitation range of 250-290 nm with emission peaks between 320 and 350 nm, which corresponds to peak T of the amino-acid like fluorescence of tryptophan, derived by *in-situ* primary production (Coble, 1996). This component (F1) was generally enriched in the SML (Figures 6, 7) with a median EF = 1.5, between a minimum EF of 0.5 and a maximum EF of 3.3. Potential loss processes of this compound are its destruction by UV light and microbial degradation (Stedmon and Markager, 2005b). F1 has also been related to protein-like fluorescence of extracellular polymeric substances (Liu and Fang, 2002). Fluorescence intensities of F1 were the lowest compared to the other fluorophores, but significantly higher in the SML compared to the ULW (Mann-Whitney Rank Sum Test, $p < 0.001$, $n = 38$). Both in SML and ULW, fluorescence intensities of F1 were positively correlated to components F3, F4 and F5 (Spearman Rank Order Correlation coefficient $C = 0.37$, $p < 0.001$, $n = 76$ with F3; $C = 0.41$, $p = 0.001$, $n = 57$ with F4; $C = 0.38$, $p < 0.001$, $n = 76$ with F5).

Component F2 had a short wavelength excitation range (250-260 nm) with emission at longer wavelengths (500-520 nm), corresponding to peak A of fulvic acids and humic acids (Stedmon and Markager, 2005a;Singh et al., 2010;Yamashita and Jaffé, 2008;Coble, 2007;Santín et al., 2009). F2 showed a regional enrichment in the SML, with highest values at the northernmost stations S2 to S3 and at stations S10_1 to S10_4 (Figure 6). F2 enrichment was not ubiquitous (Figure 7), with median EF = 1, ranging from a minimum EF = 0.5 and a maximum EF = 3.6. F2 positively correlated with bacterial abundance and temperature (Table 4) and to F3 and F5 components (Spearman Rank Order Correlation coefficient $C = 0.74$, $p < 0.001$, $n = 76$ with F3, and $C = 0.71$, $p < 0.001$, $n = 76$ with F5).

Component F3 was characterized by a clear excitation peak at 265 nm, with emission maxima in the longer wavelength range 520-540 nm. Component F3 showed a median EF = 1.1 (minimum EF = 0.3, maximum EF = 4.7), indicating a slight enrichment in the SML (Figure 7), with higher accumulations close to the coast at stations S19_2 to S1778 and at the edge of the continental shelf at stations S4 and S8 (Figure 6), in correspondence with the highest enrichment of gel particles in the SML (Engel and Galgani, 2016). In our study F3 was positively correlated with the abundance of bacteria, proteinaceous particles and increasing $SUVA_{254}$ (Table 4). It showed an inverse correlation to salinity (Table 4). Besides F1 and F2, F3 was significantly correlated to F5 (Spearman Rank Order Correlation coefficient C = 0.87, $p < 0.001$, n = 76).

Component F4 was not detectable at all stations, but showed high enrichment in the SML close to the coast and along the continental shelf at stations S10_1 to S10_4, S13_1 to S13_3, S14_1 to S15_2 (Figure 6). F4 was generally enriched in the SML (Figure 7) with median EF = 1.5 (in a minimum-maximum EF range of 0.4 – 14.9) and with significant differences in fluorescence intensity compared to the ULW (Mann-Whitney Rank Sum Test, $p < 0.001$, n = 38). F4 featured characteristics of an amino-acid like fluorophore with excitation/emission maxima in the range 250-265/284-320 in the fluorescence peak T region of tyrosine (Coble, 1996;Murphy et al., 2008;Aoki et al., 2008;Yamashita and Tanoue, 2003) and phenylalanine (Yamashita and Tanoue, 2003;Jørgensen et al., 2011) (Table 3). F4 was negatively correlated to bacterial abundance (Table 4), and to slope ratio SR with SR = (S(275-295):S(350:400)). F4 was also negatively correlated to SMHIX, indicating a low humic-acid content of this fluorophore. As for F1, it positively correlated with $SUVA_{254}$ and DHAA%-DOC (Table 4). Interestingly, F4 showed the highest fluorescence intensities among all samples.

Component F5 was quite difficult to identify, as we found no comparable spectra in the literature. It showed typical characteristics of allochtonous humic-like material with excitation/emission ranges in the peak A and C regions, which have been observed in bay and offshore waters (Mostofa et al., 2013). F5 had the highest fluorescence intensities both in the SML and ULW but was not clearly

enriched in one or the other compartment (Figure 7). EF ranged from a minimum of 0.5 and a maximum of 3, with median value = 1.1. Highest enrichments in the SML were observed at northern stations S4 and S4_2, at stations S10_1 to S10_4, and in the southern stations S20 to S1778 (Figure 6). F5 was similar in characteristics to component F3, and positively correlated to bacterial abundance and proteinaceous CSP particles (Table 4). Component F5 was also positively correlated to all other fluorophores F1, F2, F3 as described, and to F4 (Spearman Rank Order Correlation coefficient C = 0.34, p = 0.009, n = 57).

On the revisited stations, only component F1 showed a direct dependency on light exposure, significantly decreasing in fluorescence – thus concentration – with increasing global radiation intensity (r^2 = 0.56, p = 0.013, n = 10). Components F2 to F5 showed no significant change with increased irradiation (Spearmank Rank Order Correlation analysis).

3.3. Changes in CDOM properties related to the biological and physical environment

Both in the SML and ULW, CDOM optical properties as absorption coefficient a(325), S(275-295), and $SUVA_{254}$ were compared to salinity, temperature, wind speed and particulate organic carbon (POC) (Table 5). Data on POC have been described in detail in Engel and Galgani (2016). CDOM absorption coefficient a(325) decreased at higher salinity, temperature and wind speed in the SML and ULW, with stronger dependency on these physical parameters in the SML (Table 5). In both compartments, there was a positive correlation of a(325) to POC. The spectral slope parameter S(275-295), indicator for DOM molecular weight, source, and degradation processes (Helms et al., 2008), increased at higher salinity and temperature (Figure 8d) in the SML and ULW. It did not show any correlation to wind speed, but a significant negative correlation to POC in both compartments (Table 5). Moreover, an increase of bacterial and phytoplankton cells led to a lower S(275-295) both in the SML and ULW (Figures 8a, b). The dependency of S(275-295) on bacteria in the SML (Spearman Rank Order Correlation Coefficient C = - 0.59, p < 0.001, n = 35) was stronger than in the ULW (C = - 0.38, p = 0.02, n = 36), potentially indicating a higher bacterial

CDOM contribution. *S*(275-295) was also negatively correlated to phytoplankton abundance with a stronger relationship in the ULW (C = - 0.64, p = 0.001, n = 22) than in the SML (C = - 0.47, p = 0.004, n = 35). In the SML, we observed a significant decrease in *S*(275-295) with increasing abundance of gelatinous proteinaceous particles (CSP) (Figure 8c), while in the underlying water a lower *S*(275-295) was highly related to increasing concentration of polysaccharidic gels (TEP). In both SML and ULW, higher salinity, temperature and wind speed were related to lower $SUVA_{254}$ indexes, as indicators of DOM aromaticity. A positive correlation was observed instead between $SUVA_{254}$ and POC (Table 5). An increment in temperature was inversely correlated to DOM lability, and therefore bioavailability, expressed as DHAA%-DOC, indicating a higher degree of DOM degradation (Spearman Rank Order Correlation coefficient C = -0.68, $p < 0.001$, n = 29 in the SML and C = -0.66, $p < 0.001$, n = 29 in the ULW). DHAA%-DOC was also lower at higher salinity (Spearman Rank Order Correlation coefficient C = -0.42, p = 0.02, n = 29 in the SML and C = -0.63, $p < 0.001$, n = 29 in the ULW). As for *S*(275-295), we observed similar trends in SR (data not shown): SR was negatively correlated to DHAA%-DOC (Spearman Rank Order correlation coefficient C = -0.50, $p < 0.001$, n = 75) and to both gel particles abundance (Spearman Rank Order correlation coefficient C = -0.37, $p < 0.001$, n = 75 for TEP and C = -0.33, p = 0.004, n = 75 for CSP). SR did not show any significant correlation to total bacteria or phytoplankton abundance, but was significantly lower in the SML, with a median EF = 0.9 (Mann-Whitney Rank Sum Test, p = 0.013, n = 38). Furthermore, DHAA%-DOC was significantly higher in the SML (Mann-Whitney Rank Sum Test, p = 0.036, n = 38).

4. Discussion

4.1. CDOM enrichment and production in the top surface layer of the ocean

The enrichment of organic material in the SML has been mainly related to biological processes in the euphotic zone below the surface (Hardy, 1982;Liss and Duce, 2005). EBUS are among the most productive regions in the ocean and therefore interesting systems to investigate the relationship

between organic matter accumulation and SML biogeochemical properties. The Peruvian EBUS is associated with an extensive OMZ and a key region for the study of gas fluxes from the ocean (Paulmier et al., 2008;Paulmier and Ruiz-Pino, 2009;Keeling et al., 2010). The presence of an organics-enriched surface layer may strongly affect gas exchange between the marine and the atmospheric systems (Engel and Galgani, 2016). The characterization of CDOM via its optical properties adds relevant information to the organic matter composition in the SML, as it allows discriminating between terrestrial and marine sources of DOM that may be equally enriched at the surface. Moreover, it helps tracking changes in DOM "quality" deriving from higher DOM exposure to solar radiation at the sea-surface than deeper in the water column. As such, microbial and photochemical DOM turnover in the SML may contribute to the atmospheric emission of gases and chemical reactive species, and interfere with the microbial carbon loop in the ocean.

In the Peruvian EBUS, we observed a general enrichment of CDOM in the SML with respect to the ULW, based on values of the specific absorption coefficient $a(\lambda)$ measured at 325 nm. Higher values for CDOM absorbance were observed in the coastal upwelling stations characterized by lowest salinity, temperature and highest enrichment of organic components, both in the particulate and dissolved fraction (Engel and Galgani, 2016). It is commonly observed that spectral loadings of allochtonous/terrestrial-like CDOM decrease with increasing salinity (Murphy et al., 2008). However, we did not observe such trend in our samples. Instead, we found a negative correlation of amino-acid like fluorophore F1 to salinity and temperature, and no clear enrichment of humic-acid like fluorophores F2, F3 and F5 in the SML. Therefore, we think that in the SML of the study region the contribution of terrestrially derived CDOM, if any, is overwhelmed by the high productivity of the upwelling system. Organics enriched in the SML such as the amino-acidic compounds F1 and F4 found at the upwelling stations may therefore reflect other processes rather than input of allochtonous CDOM from land. DOC concentrations in the SML were related to DOC concentrations in the ULW (Engel and Galgani, 2016), and the same was true for CDOM absorption coefficient $a(325)$ (Spearman Rank Order Correlation coefficient $C = 0.82$, $p < 0.001$, n

504 = 38), implying a direct dependency of SML CDOM on the organic matter in the ULW (Zhang and
505 Yang, 2013). CDOM absorption coefficient *a*(325) as well as its spectral slope *S*(275-295) did not
506 show any correlation to changes in DOC concentrations neither in the SML, nor in the ULW, but
507 were significantly related to DOM diagenesis (DHAA%-DOC) POC, and abundance of autotrophic
508 and heterotrophic microorganisms suggesting a recent production of labile or semi-labile substrates
509 driven by *in-situ* microbial or photochemical processes in the underlying euphotic zone or at the
510 immediate sea surface. A closer look on CDOM spectral properties revealed significant differences
511 between SML and ULW. According to Helms et al. (2008), an increase in *S*(275-295) and SR
512 suggests CDOM photodegradation and decreasing molecular weight. DHAA%-DOC is used here
513 as an indicator for DOM diagenesis, thus, the extent of microbially altered DOM. The higher
514 DHAA%-DOC, the more labile, bioavailable, recent and less altered DOM in the sample. We
515 observed a negative correlation when comparing DHAA%-DOC and POC to *S*(275-295) and to SR.
516 The higher DHAA%-DOC, the lower *S*(275-295) and SR. Microorganisms adopt several strategies
517 against tough environments; the correlation between DHAA%-DOC to *S*(275-295) and SR was
518 stronger in the SML than in the ULW, suggesting an accumulation of HMW-DOM related to the
519 contribution of microorganisms directly in the SML or in the proximity due to cell lysis or
520 exudation, which has been previously proposed (Tilstone et al., 2010). Thus, the close correlations
521 of optical parameters to POC and marine gels lead to hypothesize that autochtonous CDOM
522 produced in the very surface ocean can actually be incorporated in the gelatinous organic carbon
523 pool.
524

525 **4.2. CDOM composition**

526 The analysis of EEMs allowed the identification of five fluorescent components both in the SML
527 and ULW, of which two (F1 and F4) showed an amino-acid like fluorescence of autochtonous
528 material, and three (F2, F3 and F5) had the characteristics of fulvic-acid like or humic-acid like
529 CDOM (Table 3). These classes of fluorophores are commonly found in marine environments

530 (Coble, 2007;Mostofa et al., 2013), but EEMs analyses of SML samples are scarce and up to now
531 revealed the enrichment in humic-acid like fluorophores only (Zhang and Yang, 2013). Phenolic
532 materials deriving from humic and fulvic acids transported by river drainage, and from macroalgae
533 polyphenols, are often enriched in the SML, and indicate the presence of surface slicks (Carlson,
534 1982;Carlson and Mayer, 1980). Here, we observed a significant enrichment of amino-acid like
535 fluorophores F1 and F4 with respect to ULW, in good accordance with previous reports on amino
536 acids enrichment in the SML (Kuznetsova et al., 2004;Cunliffe et al., 2013;Tilstone et al., 2010),
537 and with our own observations for the Peruvian EBUS (Engel and Galgani, 2016). F1 has shown
538 the greatest production rates during algal blooms, whereas its major sinks are UV light and
539 microbial degradation (Stedmon and Markager, 2005b). Moreover, it is assumed that F1 relates to
540 the fluorescence of amino acids still bound in the proteinaceous matrix (Stedmon and Markager,
541 2005b). Based on these previous findings and on our results (Table 4), we suggest that F1 is a
542 tryptophan-like fluorophore, originating by *in-situ* primary production, relatively labile as it features
543 an increase in fluorescence intensity correlated to increasing DHAA%-DOC, and possibly included
544 in the gel particles surface matrix. F4 showed very high fluorescence intensities compared to F1,
545 F2 and F3. In the literature, F4 has been associated to the fluorescence of amino acids in peptides
546 (Stedmon and Markager, 2005b). Similarly to F1, F4 showed a positive correlation to DHAA%-
547 DOC, as to indicate its labile nature. The aromatic content of DOM is highly responsible for its
548 photoreactivity (e.g. Mopper et al., 2014); F4 correlation to DOM lability (DHAA%-DOC) and
549 aromatic content ($SUVA_{254}$) was weaker than for F1. In our study, this may indicate F4 as an
550 intermediate product of photochemically-driven aggregation or microbial degradation of labile
551 CDOM. F4 has been linked to the fluorescence of tyrosine and phenylalanine (e.g. Coble,
552 1996;Murphy et al., 2008;Jørgensen et al., 2011) and both amino acids were enriched in the SML of
553 the Peruvian EBUS (Engel and Galgani, 2016). A recent laboratory study reported π non-covalent
554 interactions between N_2O and phenolic groups in phenylalanine and tyrosine (Cao et al., 2014).
555 Although performed in a setting non-comparable to our study area, these findings may suggest an

556 interaction of N_2O with biological macromolecules enriched in the SML of the Peruvian EBUS, and
557 thus with the exchange of N_2O between the ocean and the atmosphere (Engel and Galgani, 2016).
558 The enrichment of fluorophores F1 and F4 in the SML could be partly due to the upwelling of
559 colder nutrient-rich waters that boost primary production in the euphotic zone. Salinity and
560 temperature gradients may thus explain the variation of F1 in the SML (Table 4), reflecting local
561 upwelling and DOM production. The observed accumulation of amino-acid like CDOM may
562 additionally derive from a local microbial release within the SML itself due to cell disintegration, or
563 as protection strategy for the exposure to UVB light in a demanding environment (Ortega-Retuerta
564 et al., 2009). Mycosporine-like amino acids (MAAs), for example, serve as a natural microbial UV
565 sunscreen against photodamage (Garcia-Pichel et al., 1993) and have been observed in enriched
566 concentrations in the SML (Tilstone et al., 2010). Major losses of autochtonous protein-like
567 fluorophores in the SML may be related to photochemical and microbial degradation: negative
568 correlations of F1 and F4 to SR may hint to photochemical degradation, recalling that an increase in
569 SR is usually related to photobleached material (Helms et al., 2008). The negative correlation of F4
570 to bacterial abundance may be instead an indication of a microbial sink of this fluorophore.
571 The fulvic acid or humic acid-like components F2, F3 and F5 were ubiquitous in SML and ULW,
572 with no significant differences in fluorescence intensities between the two compartments. F2 and F3
573 have been previously observed in coastal marine environments (e.g. Jørgensen et al., 2011;Ishii and
574 Boyer, 2012). In the literature, component F2 has been characterized as of terrestrial origin,
575 allochtonous in marine environments, found in bays, rivers and coastal waters. It is assumed to
576 reflect small-sized molecules, being resistant to photodegradation, biologically not available, and
577 mainly derived from photobleached terrestrial-like humic acids in marine waters with highest
578 concentrations near the surface (Ishii and Boyer, 2012). In this study we did not find a correlation
579 of F2 to global radiation but a positive correlation to temperature and to bacterial abundance (Table
580 4). We also observed an increase of bacterial abundance with increasing sea-surface temperature,
581 which is well supported by existing literature (e.g. Morán et al., 2015). Higher temperature also

582 stimulates the activity of marine bacteria (e.g. Piontek et al., 2009). Thus, as F2 probably reflects
583 the fluorescence of highly degraded small molecules, we may characterize F2 as the ultimate
584 product of microbial CDOM degradation in the surface ocean, not bioavailable anymore. F3-like
585 fluorophores have been identified as an intermediate product of terrestrially derived DOM, still
586 subject to further photochemical degradation (Stedmon et al., 2007). Earlier studies attributed this
587 optical behavior to fulvic acid C-like components showing a peak in region A. According to Ishii
588 and Boyer (2012), F3 like components may comprise larger hydrophobic molecules that are
589 photodegradable by UV light, of terrestrial or microbial origin, biologically degraded and produced.
590 Moreover, F3 appearance has been related to apparent oxygen utilization (Yamashita et al., 2010),
591 further suggesting a microbial source of this material (Jørgensen et al., 2011). In this study, F3
592 showed a slight enrichment in the SML and was related to heterotrophic bacteria as well as to CSP
593 particles, possibly indicating its origin in microbial reworking of larger organic compounds. F5
594 showed characteristics of humic acid fluorophores, with fluorescence maximum ranges to the lower
595 end of F3 emission indicating a more pronounced CDOM alteration with respect to F3. Showing
596 similar correlations to heterotrophic bacteria and CSP, F5 may as well derive from a microbial *in-*
597 *situ* reworking of larger organic molecules both in the SML and ULW contributing to the size
598 continuum and reactivity of the gel particles pool in surface waters. In fact, a net production and
599 accumulation of humic-like CDOM in surface waters may occur in upwelling regions (Nieto-Cid et
600 al., 2005;Jørgensen et al., 2011), whereas photochemical loss is thought to be the major removal
601 mechanism of this material (e.g. Mopper and Schultz, 1993). In this study, fulvic acid/humic acid-
602 like fluorophores well correlated among each other, suggesting a common underlying origin.
603 Based on CDOM absorption and fluorescence characteristics, we propose a conceptual model for
604 the control of CDOM production and loss in the SML and ULW by microbial and photochemical
605 processes (see graphical abstract). In this model, the accumulation of CDOM in the SML is the
606 result of a) the biological production of CDOM in the ULW and deeper water column, stimulated
607 by the upwelling of nutrient-rich waters to the sunlit surface and b) the local microbial release of

608 CDOM as a response to elevated solar radiation. Previous and our own observations on amino-acid
609 fluorophores (F1, F4), as well as on the enrichment of CSP and amino acids in the SML described
610 elsewhere (Engel and Galgani, 2016), suggest a rapid turnover of fresh DOM in the sea-surface
611 itself. On one hand, microbes release fresh DOM directly within the SML or in the upper first
612 centimetres, as a consequence of high light exposure. On the other hand, and both in the SML and
613 ULW, microbial and photochemical degradation would lead to the loss of amino-acid like
614 fluorophores (F1, F4) and to the accumulation of less labile and humic-like components completely
615 degraded (F2) or still subject to further photochemical degradation (F3, F5).

616

617 **4.3. Implications for surface ocean dynamics and future perspectives**

618 Optical properties of DOM in the Peruvian EBUS revealed a SML characterized by amino-acid like
619 CDOM fluorophores. CDOM enrichment in the SML has been observed in different marine regions
620 associated with enrichment in phenolic compounds, MAAs and humic acids (Carlson, 1982;Carlson
621 and Mayer, 1980;Tilstone et al., 2010;Zhang and Yang, 2013). MAAs for example (LMW-DOM)
622 are well known as microbial sunscreen in aquatic environments (Bhatia et al., 2011;Shick and
623 Dunlap, 2002), and were observed in higher concentrations in the SML during surface slicks
624 development (Tilstone et al., 2010). Here, the accumulation of amino-acid like CDOM may have a
625 major microbial source directly in the SML or the immediate subsurface water, whereas fulvic
626 acid/humic acid-like CDOM likely originated in the sunlit zone below by microbial and
627 photochemical processing of upwelled organic material. Accumulation of amino acids in the SML
628 has been related to a reduced bacterial activity, being the SML an extreme environment where the
629 consumption of amino acids may be lower (Santos et al., 2012). A reduced bacterial activity may
630 thus also explain the amino acids enrichment in the SML of the Peruvian EBUS (Engel and
631 Galgani, 2016). We may assume that in the top layer of the ocean, and at higher extent in the SML,
632 exposure to light may have determined three main processes: 1) microbial release amino-acid like
633 CDOM as a sunscreen function, 2) increased availability of biological substrate by CDOM

photolysis and 3) further photochemical degradation of microbially-altered CDOM. Photochemistry is able to alter the HMW fraction making it more available for microbial attack (Kieber et al., 1989), but at the same time it may lead to a net loss of bioavailable substrates (Kieber, 2000). Therefore, the interplay of photochemistry and microbial activity controls the accumulation and loss of organic compounds at the sea-surface, implying consequences on gas fluxes worth deeper investigations in climate-relevant marine regions such as the OMZ off Peru. As an example, high microbial DOM respiration can lead to higher production of CO_2 in the SML (Garabétian, 1990), whereas high concentrations of isoprene may be released from photosensitized DOM reactions in the SML, proving an abiotic source of this gas uncoupled from biological production (Ciuraru et al., 2015).

It remains unclear whether in the Peruvian EBUS an increase in bioavailable carbon may have implied a higher heterotrophic respiration and CO_2 production in the SML, and this is an attractive hypothesis for future studies in this direction. It may be suggested however, that a net DOM production in the SML may take place independently of the biological productivity of the underlying waters as a sole microbial response to light exposure. We assessed the enrichment of light-absorbing proteinaceous organic material in the SML of a highly productive oceanic system, which may interfere with correct estimates of primary production from remote measurements. To conclude, we suggest that further primary production estimates may take into account the CDOM enrichment in the first centimeters of the ocean.

Acknowledgments. We would like to thank the captain and the crew of R/V Meteor during M91 cruise for the logistic support during the zodiac samplings. We also would like to thank H. Bange as chief scientist and all the scientific crew, in particular J. Roa for sampling and analysis on board and for DOC analysis back at the institute. We are very grateful to R. Flerus and T. Klüver for amino-acids measurements and flow cytometry, respectively, and to S. Manandhar and N. Bijma for microscopy analysis. The authors would like to thank K. Murphy and A. Loginova for help in

DrEEE troubleshooting and the three anonymous referees for valuable suggestions in revising this manuscript. This study has been supported by BMBF SOPRAN II and III (Surface Ocean Processes in the Anthropocene, 03F0611C-TP01 and 03F0662A-TP2.2).

This manuscript is accompanied by supplementary material.

References

- Amon, R. M. W., and Fitznar, H. P.: Linkages among the bioreactivity, chemical composition, and diagenetic state of marine dissolved organic matter, Limnol. Oceanogr., 42, 287-297, 2001.
- Aoki, S., Ohara, S., Kimura, K., Mizuguchi, H., Fuse, Y., and Yamada, E.: Characterization of Dissolved Organic Matter Released from Microcystis aeruginosa, Analytical Sciences, 24, 389-394, http://dx.doi.org/10.2116/analsci.24.389, 2008.
- Arístegui, J., Barton, E. D., Tett, P., Montero, M. F., García-Muñoz, M., Basterretxea, G., Cussatlegras, A.-S., Ojeda, A., and de Armas, D.: Variability in plankton community structure, metabolism, and vertical carbon fluxes along an upwelling filament (Cape Juby, NW Africa), Progr. Oceanogr., 62, 95-113, http://dx.doi.org/10.1016/j.pocean.2004.07.004, 2004.
- Bange, H. W.: Surface Ocean – Lower Atmosphere Study (SOLAS) in the upwelling region off the coast of Peru, Cruise No. M91, 1– 26 December, 2012, Callao (Peru), Bremen, 69 pp., 2013.
- Bange, H. W., Rapsomanikis, S., and Andreae, M. O.: Nitrous oxide cycling in the Arabian Sea, J. Geophys. Res-Oceans, 106, 1053-1065, http://dx.doi.org/10.1029/1999jc000284, 2001.
- Benner, R.: Chemical composition and reactivity, in: Biogeochemistry of marine dissolved organic matter, edited by: Hansell, D. A., and Carlson, D. J., Academic Press - Elsevier, 59-90, 2002.
- Bhatia, S., Garg, A., Sharma, K., Kumar, S., Sharma, A., and Purohit, A. P.: Mycosporine and mycosporine-like amino acids: A paramount tool against ultra violet irradiation, Pharmacognosy Reviews, 5, 138-146, http://dx.doi.org/10.4103/0973-7847.91107, 2011.
- Bigg, K. E., Leck, C., and Tranvik, L.: Particulates of the surface microlayer of open water in the central Arctic Ocean in summer, Mar. Chem., 91, 131-141, http://dx.doi.org/10.1016/j.marchem.2004.06.005, 2004.
- Blough, N. V.: Photochemistry in the sea-surface microlayer, in: The Sea Surface and Global Change, edited by: Liss, P. S., and Duce, R. A., Cambridge University Press, 383-424, 2005.
- Blough, N. V., and Del Vecchio, R.: Chromophoric DOM in the coastal environment, in: Biogeochemistry of marine dissolved organic matter, edited by: Hansell, D. A., and Carlson, D. J., Academic Press - Elsevier, 509-546, 2002.
- Bopp, L., Le Quéré, C., Heimann, M., Manning, A. C., and Monfray, P.: Climate-induced oceanic oxygen fluxes: Implications for the contemporary carbon budget, Global Biogeochemical Cycles, 16, 6-1-6-13, http://dx.doi.org/10.1029/2001GB001445, 2002.
- Bracchini, L., Dattilo, A. M., Falcucci, M., Hull, V., Tognazzi, A., Rossi, C., and Loiselle, S. A.: Competition for spectral irradiance between epilimnetic optically active dissolved and suspended matter and phytoplankton in the metalimnion. Consequences for limnology and chemistry, Photochem. Photobiol. Sci., 10, 1000-1013, http://dx.doi.org/10.1039/c0pp00291g, 2011.
- Bricaud, A., Morel, A., and Prieur, L.: Absorption by dissolved organic matter of the sea (yellow substance) in the UV and visible domains, Limnol. Oceanogr., 26, 43-53, 1981.
- Cao, Q., Gor, G. Y., Krogh-Jespersen, K., and Khriachtchev, L.: Non-covalent interactions of nitrous oxide with aromatic compounds: Spectroscopic and computational evidence for the formation of 1:1 complexes, J. Chem. Phys., 140, 144304, http://dx.doi.org/10.1063/1.4870516, 2014.
- Capone, D. G., and Hutchins, D. A.: Microbial biogeochemistry of coastal upwelling regimes in a changing ocean, Nat. Geosci., 6, 711-717, 2013.Carlson, C. A.: Production and Removal Processes, in: Biogeochemistry of Marine Dissolved Organic Matter, edited by: Hansell, D. A., and Carlson, C. A., Academic Press - Elsevier, Academic Press, 91-150, 2002.
- Carlson, D. J., and Mayer, L. M.: Enrichment of dissolved phenolic material in the surface microlayer of coastal waters, Nature, 286, 482-483, 1980.

- Carlson, D. J.: Surface microlayer phenolic enrichments indicate sea surface slicks, Nature, 296, 426-429, 1982.
- Chavez, F. P., and Messié, M.: A comparison of Eastern Boundary Upwelling Ecosystems, Progr. Oceanogr., 83, 80-96, http://dx.doi.org/10.1016/j.pocean.2009.07.032, 2009.
- Ciuraru, R., Fine, L., Pinxteren, M. v., D'Anna, B., Herrmann, H., and George, C.: Unravelling New Processes at Interfaces: Photochemical Isoprene Production at the Sea Surface, Environ. Sci. Technol., http://dx.doi.org/10.1021/acs.est.5b02388, 2015.
- Coble, P.: Characterization of marine and terrestrial DOM in seawater using excitation-emission matrix spectroscopy, Mar. Chem., 51, 325-356, 1996.
- Coble, P. G.: Marine Optical Biogeochemistry: The Chemistry of Ocean Color, Chem. Rev., 107, 402-418, 2007.
- Cunliffe, M., Upstill-Goddard, R. C., and Murrell, J. C.: Microbiology of aquatic surface microlayers, FEMS Microbiol. Rev., 35, 233-246, http://dx.doi.org/10.1111/j.1574-6976.2010.00246.x, 2011.
- Cunliffe, M., Engel, A., Frka, S., Gašparović , B., Guitart, C., Murrell, J. C., Salter, M., Stolle, C., Upstill-Goddard, R., and Wurl, O.: Sea surface microlayers: A unified physicochemical and biological perspective of the air-ocean interface, Progr. Oceanogr., 109, 104-116, http://dx.doi.org/10.1016/j.pocean.2012.08.004, 2013.
- Davis, J., and Benner, R.: Quantitative estimates of labile and semi-labile dissolved organic carbon in the western Arctic Ocean: A molecular approach, Limnol. Oceanogr., 52, 2434-2444, 2007.
- Del Giorgio, P. A., and Duarte, C. M.: Respiration in the open ocean, Nature, 420, 379-384, 2002.
- Engel, A.: Determination of Marine Gel Particles, in: Practical Guidelines for the Analysis of Seawater, edited by: Wurl, O., CRC Press, 125-142, 2009.
- Engel, A., and Galgani, L.: The organic sea-surface microlayer in the upwelling region off the coast of Peru and potential implications for air–sea exchange processes, Biogeosciences , 13, 989-1007, http://dx.doi.org/10.5194/bg-13-989-2016 , 2016.
- Galgani, L., Stolle, C., Endres, S., Schulz, K. G., and Engel, A.: Effects of ocean acidification on the biogenic composition of the sea-surface microlayer: Results from a mesocosm study, J. Geophys. Res-Oceans, 119, 7911-7924, http://dx.doi.org/10.1002/2014jc010188, 2014.
- Gao, Q., Leck, C., Rauschenberg, C., and Matrai, P. A.: On the chemical dynamics of extracellular polysaccharides in the high Arctic surface microlayer, Ocean Sci., 8, 401-418, http://dx.doi.org/10.5194/osd-9-215-2012, 2012.
- Garabétian, F.: Production de CO2 à l'interface air-mer. Une approche par l'étude des phénomènes respiratoires dans la microcouche de surface. CO2 Production at the Sea-Air Interface. An Approach by the Study of Respiratory Processes in Surface Microlayer, Int. Revue ges. Hydrobiol., 75, 219-229, http://dx.doi.org/10.1002/iroh.19900750208, 1990.
- Garcia-Pichel, F., Wingard, C. E., and Castenholz, R. W.: Evidence Regarding the UV Sunscreen Role of a Mycosporine-Like Compound in the Cyanobacterium Gloeocapsa sp, Appl. Environ. Microb., 59, 170-176, 1993.
- Garrett, W. D.: Collection of slick-forming materials from the sea surface, Limnol. Oceanogr., 10, 602-605, 1965.
- GESAMP: The Sea-Surface Microlayer and its Role in Global Change. Reports and Studies, WMO, 1995.
- Hardy, J. T.: The sea surface microlayer: Biology, chemistry and anthropogenic enrichment, Progr. Oceanogr., 11, 307-328, http://dx.doi.org/10.1016/0079-6611(82)90001-5, 1982.
- Harvey, G. W., and Burzell, L. A.: A simple microlayer method for small samples, Limnol. Oceanogr., 11, 608-614, 1972.
- Helms, J. R., Stubbins, A., Ritchie, J. D., Minor, E. C., Kieber, D. J., and Mopper, K.: Absorption spectral slopes and slope ratios as indicators of molecular weight, source, and

765 photobleaching of chromophoric dissolved organic matter, Limnol. Oceanogr., 53, 955-969,
766 2008.
767 • Huguet, A., Vacher, L., Relexans, S., Saubusse, S., Froidefond, J. M., and Parlanti, E.: Properties
768 of fluorescent dissolved organic matter in the Gironde Estuary, Org. Geochem., 40, 706-719,
769 http://dx.doi.org/10.1016/j.orggeochem.2009.03.002, 2009.
770 • Ishii, S. K. L., and Boyer, T. H.: Behavior of Reoccurring PARAFAC Components in
771 Fluorescent Dissolved Organic Matter in Natural and Engineered Systems: A Critical Review,
772 Envir. Sci. Technol., 46, 2006-2017, http://dx.doi.org/10.1021/es2043504, 2012.
773 • Jørgensen, L., Stedmon, C. A., Kragh, T., Markager, S., Middelboe, M., and Søndergaard, M.:
774 Global trends in the fluorescence characteristics and distribution of marine dissolved organic
775 matter, Mar. Chem., 126, 139-148, http://dx.doi.org/10.1016/j.marchem.2011.05.002, 2011.
776 • Kaiser, K., and Benner, R.: Biochemical composition and size distribution of organic matter at
777 the Pacific and Atlantic time-series stations, Mar. Chem., 113, 63-77,
778 http://dx.doi.org/10.1016/j.marchem.2008.12.004, 2009.
779 • Keeling, R. F., Körtzinger, A., and Gruber, N.: Ocean Deoxygenation in a Warming World,
780 Annu. Rev. Mar. Sci., 2, 199-229, http://dx.doi.org/10.1146/annurev.marine.010908.163855,
781 2010.
782 • Kieber, D. J., McDaniel, J., and Mopper, K.: Photochemical source of biological substrates in
783 sea water: implications for carbon cycling, Nature, 341, 637-639, 1989.
784 • Kieber, D. J.: Photochemical production of biological substrates, in: The effects of UV radiation
785 in the marine environment, edited by: De Mora, S. et al. Cambridge Environmental Chemistry
786 Series (No. 10), Cambridge University Press, 130-148, 2000.
787 • Kuznetsova, M., Lee, C., and Aller, J.: Enrichment of amino acids in the sea surface microlayer
788 at coastal and open ocean sites in the North Atlantic Ocean, Limnol. Oceanogr., 49, 1605-1619,
789 2004.
790 • Lachkar, Z., and Gruber, N.: What controls biological production in coastal upwelling systems?
791 Insights from a comparative modeling study, Biogeosciences, 8, 2961-2976,
792 http://dx.doi.org/10.5194/bg-8-2961-2011, 2011.
793 • Lawaetz, A. J., and Stedmon, C. A.: Fluorescence Intensity Calibration Using the Raman Scatter
794 Peak of Water, Appl. Spectrosc., 63, 936-940, http://dx.doi.org/10.1366/000370209788964548,
795 2009.
796 • Liss, P. S., and Duce, R. A.: The Sea Surface and Global Change, Cambridge University Press,
797 2005.
798 • Liu, H., and Fang, H. H. P.: Characterization of electrostatic binding sites of extracellular
799 polymers by linear programming analysis of titration data, Biotechnol. Bioeng., 80, 806-811,
800 http://dx.doi.org/10.1002/bit.10432, 2002.
801 • Loginova, A. N., Borchard, C., Meyer, J., Hauss, H., Kiko, R., and Engel, A.: Effects of nitrate
802 and phosphate supply on chromophoric and fluorescent dissolved organic matter in the Eastern
803 Tropical North Atlantic: a mesocosm study, Biogeosciences, 12, 6897-6914, doi:10.5194/bg-12-
804 6897-2015, 2015.
805 • Loiselle, S., Vione, D., Minero, C., Maurino, V., Tognazzi, A., Dattilo, A. M., Rossi, C., and
806 Bracchini, L.: Chemical and optical phototransformation of dissolved organic matter, Water
807 Res., 46, 3197-3207, http://dx.doi.org/10.1016/j.watres.2012.02.047, 2012.
808 • Matrai, P. A., Tranvik, L., Leck, C., and Knulst, J. C.: Are high Arctic surface microlayers a
809 potential source of aerosol organic precursors?, Mar. Chem., 108, 109-122,
810 http://dx.doi.org/10.1016/j.marchem.2007.11.001, 2008.
811 • Miller, W. L., and Zepp, R. G.: Photochemical production of dissolved inorganic carbon from
812 terrestrial organic matter: Significance to the oceanic organic carbon cycle, Geophys. Res. Lett.,
813 22, 417-420, http://dx.doi.org/10.1029/94gl03344, 1995.

- Mopper, K., and Schultz, C. A.: Fluorescence as a possible tool for studying the nature and water column distribution of DOC components, Mar. Chem., 41, 229-238, http://dx.doi.org/10.1016/0304-4203(93)90124-7, 1993.
- Mopper, K., Kieber, D. J., and Stubbins, A.: Marine Photochemistry of Organic Matter: Processes and Impacts, in: Biogeochemistry of marine dissolved organic matter, Second Edition, edited by: Hansell, D. A., and Carlson, D. J., Academic Press - Elsevier, 390-450, http://dx.doi.org/10.1016/B978-0-12-405940-5.00008-X, 2014.
- Morán, X. A. G., Alonso-Sáez, L., Nogueira, E. Ducklow, H. W., González, N. López-Urrutia, Á., Díaz-Pérez, L., Calvo-Díaz, A., Arandia-Gorostidi, N., and Huete-Stauffer, T. M.: More, smaller bacteria in response to ocean's warming?, Proc. R. Soc. B., 282, 20150371, http://dx.doi.org/10.1098/rspb.2015.0371, 2015.
- Mostofa, K. G., Liu, C.-q., Yoshioka, T., Vione, D., Zhang, Y., and Sakugawa, H.: Fluorescent Dissolved Organic Matter in Natural Waters, in: Photobiogeochemistry of Organic Matter, edited by: Mostofa, K. M. G., Yoshioka, T., Mottaleb, A., and Vione, D., Environmental Science and Engineering, Springer Berlin Heidelberg, 429-559, 2013.
- Muller-Karger, F. E., Varela, R., Thunell, R., Luerssen, R., Hu, C., and Walsh, J. J.: The importance of continental margins in the global carbon cycle, Geophys. Res. Lett., 32, n/a-n/a, http://dx.doi.org/10.1029/2004GL021346, 2005.
- Murphy, K. R., Stedmon, C. A., Waite, T. D., and Ruiz, G. M.: Distinguishing between terrestrial and autochthonous organic matter sources in marine environments using fluorescence spectroscopy, Mar. Chem., 108, 40-58, http://dx.doi.org/10.1016/j.marchem.2007.10.003, 2008.
- Murphy, K. R., Stedmon, C. A., Graeber, D., and Bro, R.: Fluorescence spectroscopy and multi-way techniques. PARAFAC, Anal. Methods, 5, 6557-6566, http://dx.doi.org/10.1039/c3ay41160e, 2013.
- Nelson, N. B., and Siegel, D. A.: The Global Distribution and Dynamics of Chromophoric Dissolved Organic Matter, Annual Review of Marine Science, 5, 447-476, http://dx.doi.org/10.1146/annurev-marine-120710-100751, 2013.
- Nieto-Cid, M., Ã□lvarez-Salgado, X. A., Gago, J., and PÃ©rez, F. F.: DOM fluorescence, a tracer for biogeochemical processes in a coastal upwelling system (NW Iberian Peninsula), Mar. Ecol. Prog. Ser., 297, 33-50, http://dx.doi.org/10.3354/meps297033, 2005.
- Ortega-Retuerta, E., Passow, U., Duarte, C. M., and Reche, I.: Effects of ultraviolet B radiation on (not so) transparent exopolymer particles, Biogeosciences, 6, 3071-3080, http://dx.doi.org/10.5194/bg-6-3071-2009, 2009.
- Paulmier, A., Ruiz-Pino, D., and Garcon, V.: The oxygen minimum zone (OMZ) off Chile as intense source of CO2 and N2O, Cont. Shelf Res. , 28, 2746-2756, http://dx.doi.org/10.1016/j.csr.2008.09.012, 2008.
- Paulmier, A., and Ruiz-Pino, D.: Oxygen minimum zones (OMZs) in the modern ocean, Progr. Oceanogr., 80, 113-128, http://dx.doi.org/10.1016/j.pocean.2008.08.001, 2009.
- Paulmier, A., Ruiz-Pino, D., and Garçon, V.: CO2 maximum in the oxygen minimum zone (OMZ), Biogeosciences, 8, 239-252, http://dx.doi.org/10.5194/bg-8-239-2011, 2011.
- Piontek, J., Händel, N., Langer, G., Wohlers, J., Riebesell, U., and Engel, A.: Effects of rising temperature on the formation and microbial degradation of marine diatom aggregates, Aquat. Microb. Ecol., 54, 305–318, 2009.
- Riebesell, U., Kortzinger, A., and Oschlies, A.: Sensitivities of marine carbon fluxes to ocean change, Proc. Natl. Acad. Sci. U.S.A., 106, 20602-20609, http://dx.doi.org/10.1073/pnas.0813291106, 2009.
- Rosenberg, R., Arntz, W. E., de Flores, E. C., Flores, L. A., Carbajal, G., Finger, I., and Tarazona, J.: Benthos biomass and oxygen deficiency in the upwelling system off Peru, Journal of Marine Research, 41, 263-279, http://dx.doi.org/10.1357/002224083788520153, 1983.
- Santín, C., Yamashita, Y., Otero, X. L., Álvarez, M. Á., and Jaffé, R.: Characterizing humic substances from estuarine soils and sediments by excitation-emission matrix spectroscopy and

parallel factor analysis, Biogeochemistry, 96, 131-147, http://dx.doi.org/10.1007/s10533-009-9349-1, 2009.

- Santos, A. L., Oliveira, V., Baptista, I., Henriques, I., Gomes, N. C., Almeida, A., Correia, A., and Cunha, A.: Effects of UV-B radiation on the structural and physiological diversity of bacterioneuston and bacterioplankton, Appl. Environ. Microbiol., 78, 2066-2069, http://dx.doi.org/10.1128/aem.06344-11, 2012.
- Schneider-Zapp, K., Salter, M. E., Mann, P. J., and Upstill-Goddard, R. C.: Technical Note: Comparison of storage strategies of sea surface microlayer samples, Biogeosciences, 10, 4927-4936, http://dx.doi.org/10.5194/bg-10-4927-2013, 2013.
- Senesi, N.: Molecular and quantitative aspects of the chemistry of fulvic acid and its interactions with metal ions and organic chemicals, Anal. Chim. Acta, 232, 77-106, http://dx.doi.org/10.1016/S0003-2670(00)81226-X, 1990.
- Senesi, N., Miano, T. M., Provenzano, M. R., and Brunetti, G.: Characterization, differentiation and classification of humic substances by fluorescence spectroscopy, Soil Science, 152, 259-271, 1991.
- Shick, J. M., and Dunlap, W. C.: Mycosporine-like Amino Acids and related Gadusols: Biosynthesis, Accumulation, and UV-Protective Functions in Aquatic Organisms, Annu. Rev. Physiol., 64, 223-262, http://dx.doi.org/10.1146/annurev.physiol.64.081501.155802, 2002.
- Singh, S., D'Sa, E. J., and Swenson, E. M.: Chromophoric dissolved organic matter (CDOM) variability in Barataria Basin using excitation–emission matrix (EEM) fluorescence and parallel factor analysis (PARAFAC), Sci. Total Environ., 408, 3211-3222, http://dx.doi.org/10.1016/j.scitotenv.2010.03.044, 2010.
- Solomon, S., Qin, D., Manning, M., Chen, Z., Marquis, M., Averyt, K. B., Tignor, M., and Miller, H. L.: Climate Change 2007: The Physical Science Basis. Contribution of Working Group I to the Fourth Assessment Report of the Intergovernmental Panel on Climate Change, Cambridge, United Kingdom and New York, NY, USA, Cambridge University Press, 2007.
- Stedmon, C. A., and Markager, S.: Resolving the variability in dissolved organic matter fluorescence in a temperate estuary and its catchment using PARAFAC analysis, Limnol. Oceanogr., 50, 686-697, http://dx.doi.org/10.4319/lo.2005.50.2.0686, 2005a.
- Stedmon, C. A., and Markager, S.: Tracing the production and degradation of autochthonous fractions of dissolved organic matter by fluorescence analysis, Limnol. Oceanogr., 50, 1415-1426, http://dx.doi.org/10.4319/lo.2005.50.5.1415, 2005b.
- Stedmon, C. A., Markager, S., Tranvik, L., Kronberg, L., Slätis, T., and Martinsen, W.: Photochemical production of ammonium and transformation of dissolved organic matter in the Baltic Sea, Mar. Chem., 104, 227-240, http://dx.doi.org/10.1016/j.marchem.2006.11.005, 2007.
- Stedmon, C. A., and Bro, R.: Characterizing dissolved organic matter fluorescence with parallel factor analysis: a tutorial, Limnol. Ocenogr. Methods, 6, 572-579, 2008.
- Stramma, L., Johnson, G. C., Sprintall, J., and Mohrholz, V.: Expanding Oxygen-Minimum Zones in the Tropical Oceans, Science, 320, 655-658, http://dx.doi.org/10.1126/science.1153847, 2008.
- Swan, C. M., Siegel, D. A., Nelson, N. B., Carlson, C. A., and Nasir, E.: Biogeochemical and hydrographic controls on chromophoric dissolved organic matter distribution in the Pacific Ocean, Deep-Sea Res. Pt I, 56, 2175-2192, http://dx.doi.org/10.1016/j.dsr.2009.09.002, 2009.
- Tilstone, G. H., Airs, r. L., Vicente, V. M., Widdicombe, C., and Llewellyn, C.: High concentrations of mycosporine-like amino acids and colored dissolved organic matter in the sea surface microlayer off the Iberian Peninsula, Limnol. Oceanogr., 55, 1835-1850, http://dx.doi.org/10.4319/lo.2010.55.5.1835, 2010.
- Weishaar, J. L., Aiken, G. R., Bergamaschi, B. A., Fram, M. S., Fujii, R., and Mopper, K.: Evaluation of Specific Ultraviolet Absorbance as an Indicator of the Chemical Composition and Reactivity of Dissolved Organic Carbon, Envir. Sci. Technol., 37, 4702-4708, http://dx.doi.org/10.1021/es030360x, 2003.

- Wurl, O., and Holmes, M.: The gelatinous nature of the sea-surface microlayer, Mar. Chem., 110, 89-97, http://dx.doi.org/10.1016/j.marchem.2008.02.009, 2008.
- Yamashita, Y., and Tanoue, E.: Chemical characterization of protein-like fluorophores in DOM in relation to aromatic amino acids, Mar. Chem., 82, 255-271, http://dx.doi.org/10.1016/s0304-4203(03)00073-2, 2003.
- Yamashita, Y., and Jaffé, R.: Characterizing the Interactions between Trace Metals and Dissolved Organic Matter Using Excitation−Emission Matrix and Parallel Factor Analysis, Envir. Sci. Technol., 42, 7374-7379, http://dx.doi.org/10.1021/es801357h, 2008.
- Yamashita, Y., Cory, R. M., Nishioka, J., Kuma, K., Tanoue, E., and Jaffé, R.: Fluorescence characteristics of dissolved organic matter in the deep waters of the Okhotsk Sea and the northwestern North Pacific Ocean, Deep-Sea Res. Pt II, 57, 1478-1485, http://dx.doi.org/10.1016/j.dsr2.2010.02.016, 2010.
- Zhang, J., and Yang, G.: Chemical properties of colored dissolved organic matter in the sea-surface microlayer and subsurface water of Jiaozhou Bay, China in autumn and winter, Acta Oceanol. Sin., 32, 26-39, http://dx.doi.org/10.1007/s13131-013-0306-4, 2013.
- Zhang, Z., Liu, L., Wu, Z., Li, J., and Ding, H.: Physicochemical Studies of the Sea Surface Microlayer: I. Thickness of the Sea Surface Microlayer and Its Experimental Determination, J. Colloid Interface Sci., 204, 294-299, http://dx.doi.org/10.1006/jcis.1998.5538, 1998.
- Zsolnay, A., Baigar, E., Jimenez, M., Steinweg, B., and Saccomandi, F.: Differentiating with fluorescence spectroscopy the sources of dissolved organic matter in soils subjected to drying, Chemosphere, 38, 45-50, http://dx.doi.org/10.1016/S0045-6535(98)00166-0, 1999.

Tables

Table 1. Data on average, maximum and minimum salinity, water temperature, global radiation and wind speed during M91. Data were retrieved from Dship data server of R/V Meteor.

	Salinity [PSU]	Temperature [°C]	Global Radiation [W m^{-2}]	Wind Speed [m s^{-1}]
Average	34.9	19.2	539	5.5
SD	0.2	1.7	352	2.1
Min	34.4	15.9	10	0.6
Max	35.3	21.9	1088	9.0

Table 2. Stations with multiple measurements. Metadata with date, local and UTC time of sampling, coordinates, and average global radiation retrieved from Dship data server of R/V Meteor.

Station Ship ID	Nr.	Station nr.	Samples	Date	Time [UTC]	Time [Local]	Lat, S [°]	Long, W [°]	Average Global Radiation [W m^{-2}]
1733-5	1	S7	sml/ulw	08-12-12	11:30	6:30	9°31.258'	79°17.886'	10
1733-9		S7_2	sml/ulw	08-12-12	19:45	14:45	9°32.75'	79°18.43	837
1752-2	2	S12_1	sml/ulw	13-12-12	12:00	7:00	12°55.20'	78°.42.00'	380.5
1752-7		S12_2	sml/ulw	13-12-12	20:30	15:30	12°59.79'	78°.41.00'	704.5
1752-9		S12_3	sml/ulw	13-12-12	23:10	18:10	12°55.20'	78°.42.03'	47
1764-4	3	S16_1	sml/ulw	17-12-12	12:40	7:40	14°7.708'	76°52.759'	381
1764-6		S16_2	sml/ulw	17-12-12	17:40	12:40	14°11.11'	76°55.95'	1043
1764-9		S16_3	sml/ulw	17-12-12	22:00	17:00	14°11.10'	76°55.99'	161.5
1777-2	4	S20	sml/ulw	22-12-12	18:00	13:00	15°31.174'	75°36.015'	1088
1777-10		S20_2	sml/ulw	23-12-12	15:00	10:00	15°36.42'	75°38.60'	1046

Table 3. Fluorescent components identified in this study in both SML and ULW samples, according to their Ex/Em maxima ranges (nm), maximum fluorescence intensity range Fmax (R.U.), corresponding peaks individuated in previous studies (peak name, region, Ex/Em ranges) and properties.

Components of this study	Ex/Em maxima [nm]	Fmax range [R.U.]	Literature peak name (region, Ex/Em)	Reference	Properties
F1	250-290/ 320-350	0.001-0.228	(T) (275/340)	A	Protein-like fluorescence of tryptophan Autochtonous material. Source: in situ primary production.
			6(B) (280/338)	B	Protein-like fluorescence of tryptophan, autochtonous material. Source: algal growth. Sink: microbial reworking, UVB.
			T (280-285/340-350)	C	Protein-like, extracted from EPS.
F2	250-260/ 500-520	0.048-1.709	2(A) (250/504)	D	Fulvic acid C-like allochtononus material present in all environments. Terrestrial/autochthonous fulvic acid fluorophore group.
			1(A) (250/520)	E	Fulvic acid C-like. Bay waters, allochtonous.
			2(A) (<260/>500)	F	Humic Acid C-like, river and coastal waters, allochtonous. Terrestrial humic.
			1(A) (<230-260/400-500)	G	Small sized molecules, photoresistant and biologically not available. Source: photochemistry, terrestrially derived humic acids in marine waters, highest concentrations near the water surface.
			2(A?) (250/504)	H	UVA humic-like, fulvic acid, terrestrial, autochtonous.
			C2(-) (256/>500)	I	Humic acid C-like, estuaries of the Iberian peninsula, allochtonous.
F3	265/520-540	0.019-1.640	2(A+C) (<240-275/434-520)	G	Larger molecules, hydrophobic compounds, photodegradable by UVA light. Source: terrestrial or microbial, intermediate inputs of minimal exposure to sunlight, biologically degraded and produced.
			C1 (~275/400-550)	L	Humic-like CDOM microbially produced.
			1(A/C) (<260/466)	O	Humic-like CDOM oxidized *in situ* by microbial processes.
F4	250-265/ 284-320	0.002-6.507	(T) (275/300)	J	Protein-like fluorescence of tyrosine. Autochtonous material. Source: in situ primary production, North Pacific and Atlantic Ocean.
			4(T) (275/306(338))	B	Fluorescence of tryptophan and tyrosine in peptides. Greatest production rates during establishment of algal bloom. Source: algae in exponential growth phase. Sinks: not identified (microbial uptake or aggregation?)
			(B) (275/310)	A	Tyrosine-like, marine waters, autochtonous.
			C(T) (270-290/250-365)	K	Autochtonous protein-like hydrophobic acid fraction from phytoplankton cultures.
			C3(T)	L	Protein-like fluorescence of phenylanine.
			Standard (255-265/284-285)	M	Protein-like fluorescence of phenylanine. Source: standard.
			(B) (265-280/293-313)	M	Protein-like fluorescence of tyrosine. Source: autochtonous.
F5	270-275/	0.023-	(A,C)	N	Humic acid C-like or A-like, allochtonous

	540-550	1.714	(<260-270/>508)	material in bay and marine waters.

References:

A: Coble, 1996, Marine Chemistry 51:325-346
B: Stedmon and Markager, 2005b, Limonology and Oceanography 50(5):1415-1426
C: Liu and Fang 2002, Biotechnology and Bioengineering 80(7):806-811
D: Stedmon and Markager, 2005a, Limonology and Oceanography 50(2):686-697
E: Singh et al. 2010, Science of The Total Environment 408(16):3211-3222
F: Yamashita and Jaffè, 2008, Environmental Science and Technology 42:7374–7379
G: Ishii and Boyer, 2012, Environmental Science and Technology 46:2006-2017
H: Coble, 2007, Chemical Reviews 107(2):402:418
I: Santin et al. 2009, Biogeochemistry 96:131–147
J: Murphy et al. 2008, Marine Chemistry 108 (1-2):40-58
K: Aoki et al. 2008, Analytical Sciences 24(11):1461-1467
L: Jørgensen et al. 2011, Marine Chemistry 126:139-148
M: Yamashita and Tanoue, 2003, Marine Chemistry 82:255–271
N: Mostofa et al. 2013, In: Photobiogeochemistry of Organic Matter, Edited by Mostofa, K.M.G, Liu, C., Yoshioka,T., Vione, D., Zhang, Y., Sakugawa H., Springer Berlin Heidelberg, pp:429-559
O: Yamashita et al. 2010, Deep Sea Research II 57: 1478-1485

Table 4. Spearman Rank Order Correlation coefficients (*C*) between fluorescent components (F1-5) and total bacterial and phytoplankton cells, TEP and CSP particles, $SUVA_{254}$, *S*(275-295), *SR*, *a*(325), DHAA%-DOC, SMHIX, salinity and temperature measured in our study, both in the SML and ULW. Statistical significance was accepted for $p < 0.05$. *n* = number of samples. Only statistically significant correlations are shown. Bold characters indicate negative correlations.

Component [R.U.]	Statistics	Bacteria [cells mL^{-1}]	Phytoplankton [cells mL^{-1}]	TEP [L^{-1}]	CSP [L^{-1}]	$SUVA_{254}$ [mg C L^{-1} m^{-1}]	*S*(275-295) [nm^{-1}]	*SR*	*a*(325) [m^{-1}]	DHAA%-DOC [%]	SMHIX	Salinity [psu]	Temperature [° C]
F1	*C* *p* *n*	-	*0.285* *0.031* *57*	*0.281* *0.014* *76*		*0.620* *< 0.001* *76*	***- 0.257*** ***0.025*** ***76***	***- 0.387*** ***< 0.001*** ***75***	*0.406* *< 0.001* *76*	*0.696* *< 0.001* *76*	***- 0.342*** ***0.003*** ***76***	***- 0.261*** ***0.023*** ***76***	***- 0.323*** ***0.004*** ***76***
F2	*C* *p* *n*	*0.393* *< 0.001* *71*	-	-	-	-	-	-	-	-	*0.225* *0.050* *76*	-	*0.238* *0.038* *76*
F3	*C* *p* *n*	*0.355* *0.002* *71*	-	-	*0.411* *< 0.001* *76*	*0.305* *0.007* *76*	***- 0.221*** ***0.055*** ***76***	***- 0.226*** ***0.051*** ***76***	-	-	-	***- 0.273*** ***0.017*** ***76***	-
F4	*C* *p* *n*	***- 0.409*** ***0.003*** ***52***	-	-	-	*0.346* *0.008* *56*	-	***- 0.410*** ***0.002*** ***56***	-	*0.392* *0.008* *56*	***- 0.536*** ***< 0.001*** ***57***	-	-
F5	*C* *p* *n*	*0.270* *0.023* *71*	-	-	*0.402* *< 0.001* *76*	-	-	-	-	-	-	-	-

Table 5. Spearman Rank Order Correlation (C) between CDOM optical properties both in the SML and ULW with salinity (C_{PSU}), water temperature (C_T), wind speed (C_U) and particulate organic carbon (C_{POC}). Significant correlations ($p < 0.01$) are marked in bold (except [a] = $p < 0.05$). n is the number of samples, except * = 36 samples.

SML	C_{PSU}	C_T	C_U	C_{POC}	n
CDOM a(325)	**-0.420**	**-0.728**	**-0.535**	**0.579**	38
S(275-295)	**0.640**	**0.616**	0.318	**-0.597**	38
$SUVA_{254}$	**-0.380**[a]	**-0.634**	**-0.460**	**0.537**	38
ULW	C_{PSU}	C_T	C_U	C_{POC}	n
CDOM a(325)	**-0.329**[a]	**-0.637**	**-0.386**[a]	**0.656***	38
S(275-295)	**0.493**	**0.613**	0.24	**-0.622***	38
$SUVA_{254}$	**-0.326**[a]	**-0.458**	**-0.324**[a]	**0.495***	38

Figures' legend

Figure 1. Maps showing all sampled stations. Stations with multiple measurements are: (1) S7/7_2, (2) S12_1/3 and S12_2, (3) S16_1, S16_2/3, (4) S20 and S20_2. The locations of S7 and S7_2; S12_1 and S12_3; S16_2 and S16_3 coincide, as sampling was performed at different times.

Figure 2. CDOM absorption coefficient $a(325)$, [m^{-1}], in SML and underlying water (ULW) and spectral slope parameter between 275 and 295 nm, $S(275\text{-}295)$, [nm^{-1}].

Figure 3. Box and Whiskers plot of enrichment factors for CDOM absorption coefficient $a(325)$, aromaticity (SUVA254), DOM diagenetic state (DHAA%-DOC), spectral slope $S(275\text{-}295)$, and modified surface microlayer humification index (SMHIX). The horizontal lines of the boxes represent 25%, 50% (median) and 75% percentiles (from bottom to top). In the boxes, crosses represent the mean. Whiskers represent minimum and maximum values, and circles are outliers. Outliers are staggered to better visualize them. To identify the station, see outliers' labels and color legend. For $a(325)$, SUVA254 and $S(275\text{-}295)$ $n = 38$. For SMHIX, $n = 37$ and for DHAA%-DOC $n = 29$.

Figure 4. Enrichment factors (EF) in the Peruvian upwelling region. From the top left, EF for absorption coefficient measured at 325 nm both in SML and ULW, spectral slope parameter $S(275\text{-}295)$ as indicator for changes in DOM molecular weight, SUVA254 as indicator for DOM aromatic content, DHAA%-DOC as indicator of DOM lability, and SMHIX as indicator of humic content of DOM.

Figure 5. (Above) Contour plots of five fluorescent components as identified by PARAFAC analysis and (below) relative spectral loadings of overlaid spectra for the 5-components model validated with 3 split comparisons. The axes of contour plots have been scaled to better visualize the fluorescence intensities (R.U.). A figure with the complete spectrum is included in the supplementary material (Figure S3). The dashed black line in the spectral loadings indicates excitation maxima for each component, the solid black line indicates emission peaks.

Figure 6. Distribution of enrichment factors (EF) for fluorescent components F1, F2, F3, F4, F5 identified in this study. Maximum EF for F4 has been recorded at station S10_2, with a value of 14.9. For visualization purposes, this data point is not included in the figure and fluorescence intensities have been scaled down to a maximum EF = 6.

Figure 7. Box and Whiskers plot of enrichment factors for fluorescent components F1, F2, F3, F4 and F5. The horizontal lines of the boxes represent 25%, 50% (median) and 75% percentiles (from bottom to top). In the boxes, crosses represent the mean. Whiskers represent minimum and maximum values, and circles are outliers. Outliers are staggered to better visualize them. To identify the station, see outliers' labels and color legend. For F4, n = 24. For all other components, n = 38.

Figure 8a-d. (a) Linear regression between bacterial abundance [10^6 cells mL^{-1}] and spectral slope S(275-295) [nm^{-1}] in SML and ULW. (b) Linear regression (ULW) and Spearman Rank Order Correlation (SML) between phytoplankton abundance [10^4 cells mL^{-1}] and spectral slope S(275-295) [nm^{-1}]. (c) Linear regression between CSP abundance [10^8 particles L^{-1}] and spectral slope S(275-295) [nm^{-1}] in the SML and between TEP abundance [10^8 particles L^{-1}] and spectral slope S(275-295) [nm^{-1}] in the ULW. (d) Linear regression between temperature [°C] and S(275-295) [nm^{-1}] in SML and ULW. Black triangles: SML, open dots: ULW.

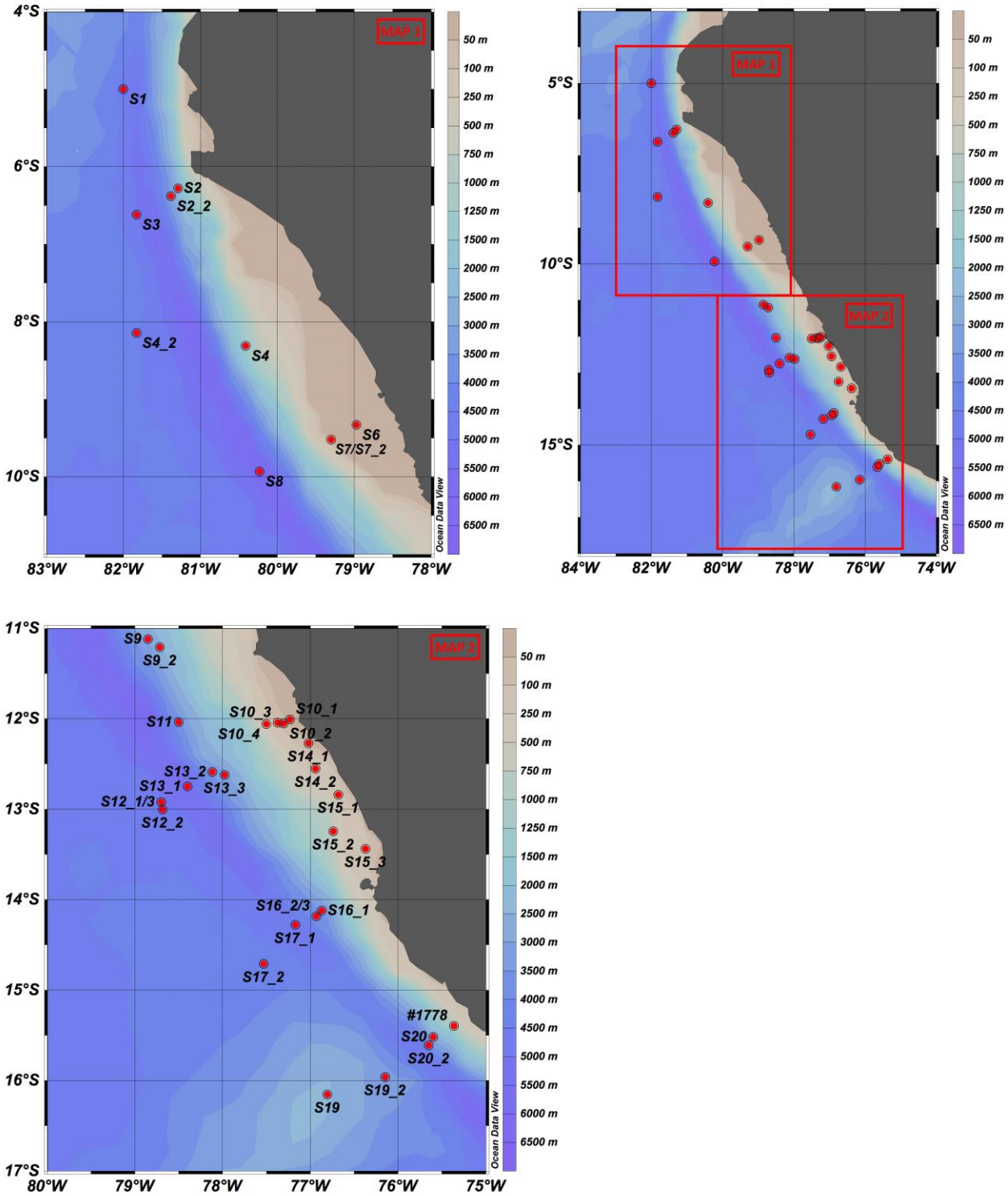
MAP 1
S1
S2
S2_2
S3
S4_2
S4
S6
S7/S7_2
S8
MAP 1
MAP 2
MAP 3
S9
S9_2
S10_3
S10_1
S11
S10_4
S10_2
S14_1
S13_2
S14_2
S13_1
S13_3
S12_1/3
S15_1
S12_2
S15_2
S15_3
S16_2/3
S16_1
S17_1
S17_2
#1778
S20
S20_2
S19_2
S19
Ocean Data View
50 m
100 m
250 m
500 m
750 m
1000 m
1250 m
1500 m
2000 m
2500 m
3000 m
3500 m
4000 m
4500 m
5000 m
5500 m
6000 m
6500 m
4°S
6°S
8°S
10°S
83°W
82°W
81°W
80°W
79°W
78°W
5°S
10°S
15°S
84°W
82°W
80°W
78°W
76°W
74°W
11°S
12°S
13°S
14°S
15°S
16°S
17°S
80°W
79°W
78°W
77°W
76°W
75°W

Figure 8

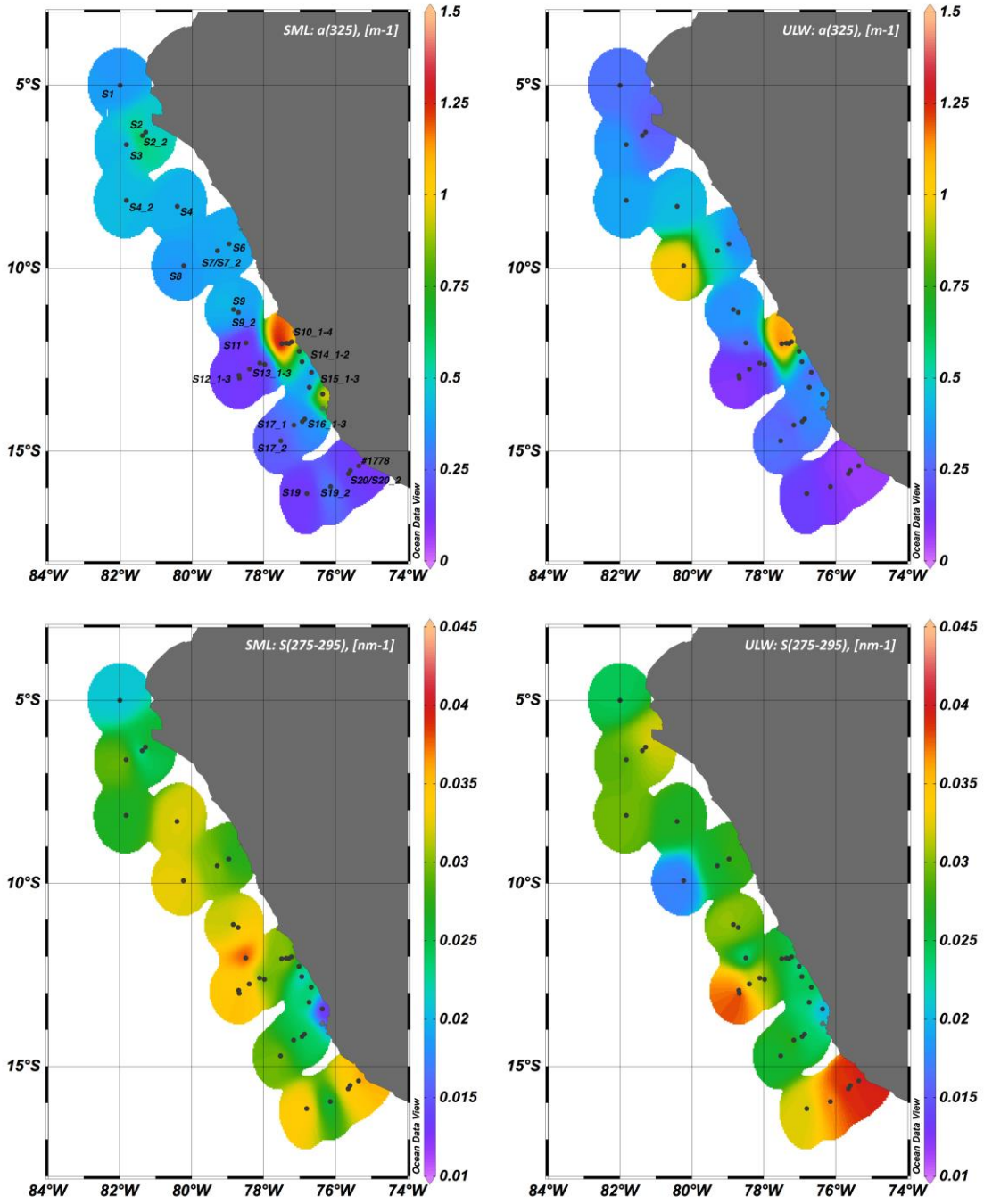
SML: a(325), [m-1]
ULW: a(325), [m-1]
SML: S(275-295), [nm-1]
ULW: S(275-295), [nm-1]
5°S
10°S
15°S
84°W
82°W
80°W
78°W
76°W
74°W
1.5
1.25
1
0.75
0.5
0.25
0
0.045
0.04
0.035
0.03
0.025
0.02
0.015
0.01
Ocean Data View

Figure 9

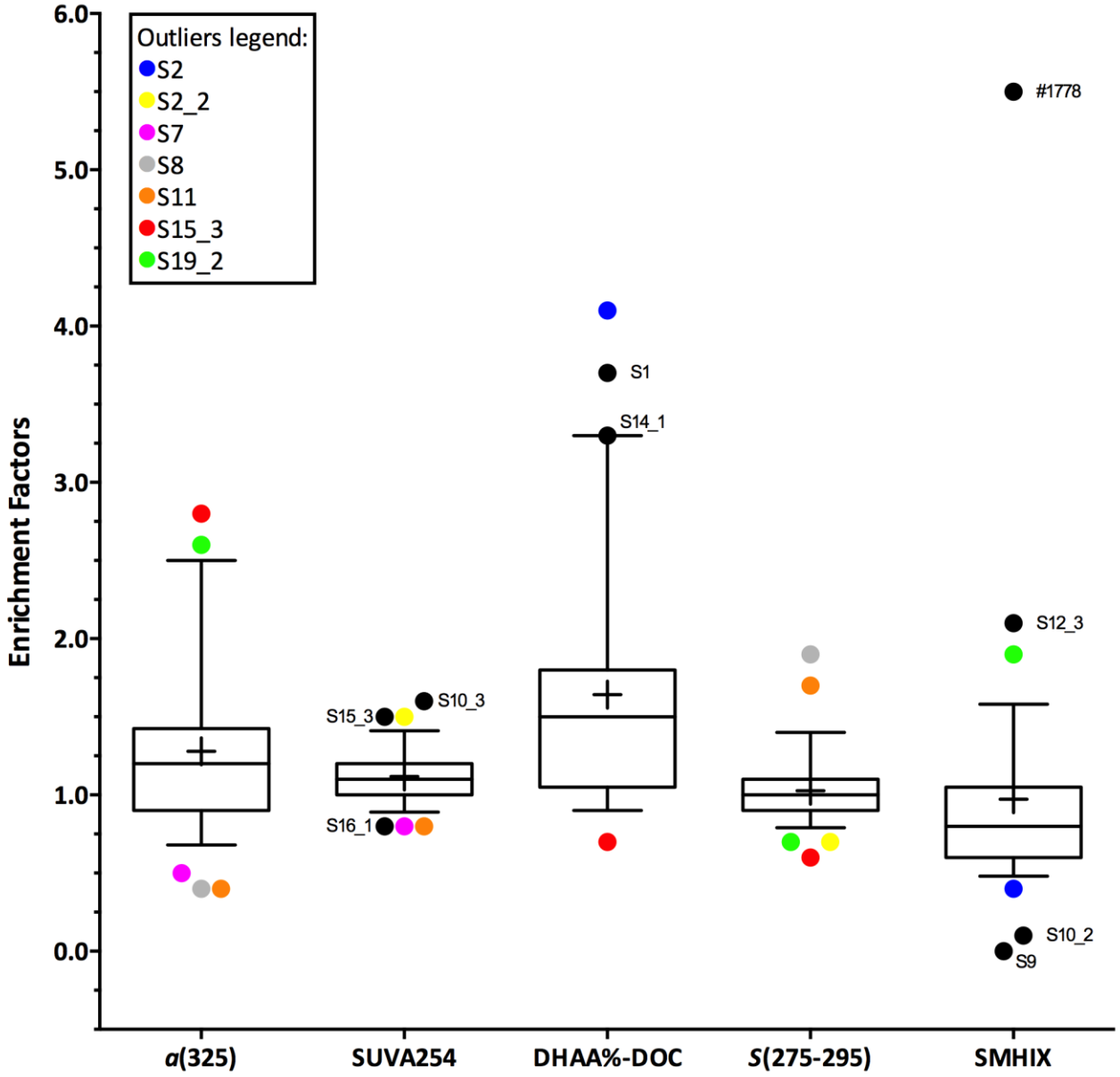
Outliers legend:
S2
S2_2
S7
S8
S11
S15_3
S19_2
Enrichment Factors
6.0
5.0
4.0
3.0
2.0
1.0
0.0
#1778
S1
S14_1
S12_3
S10_3
S15_3
S16_1
S10_2
S9
a(325)
SUVA254
DHAA%-DOC
S(275-295)
SMHIX

Figure 10

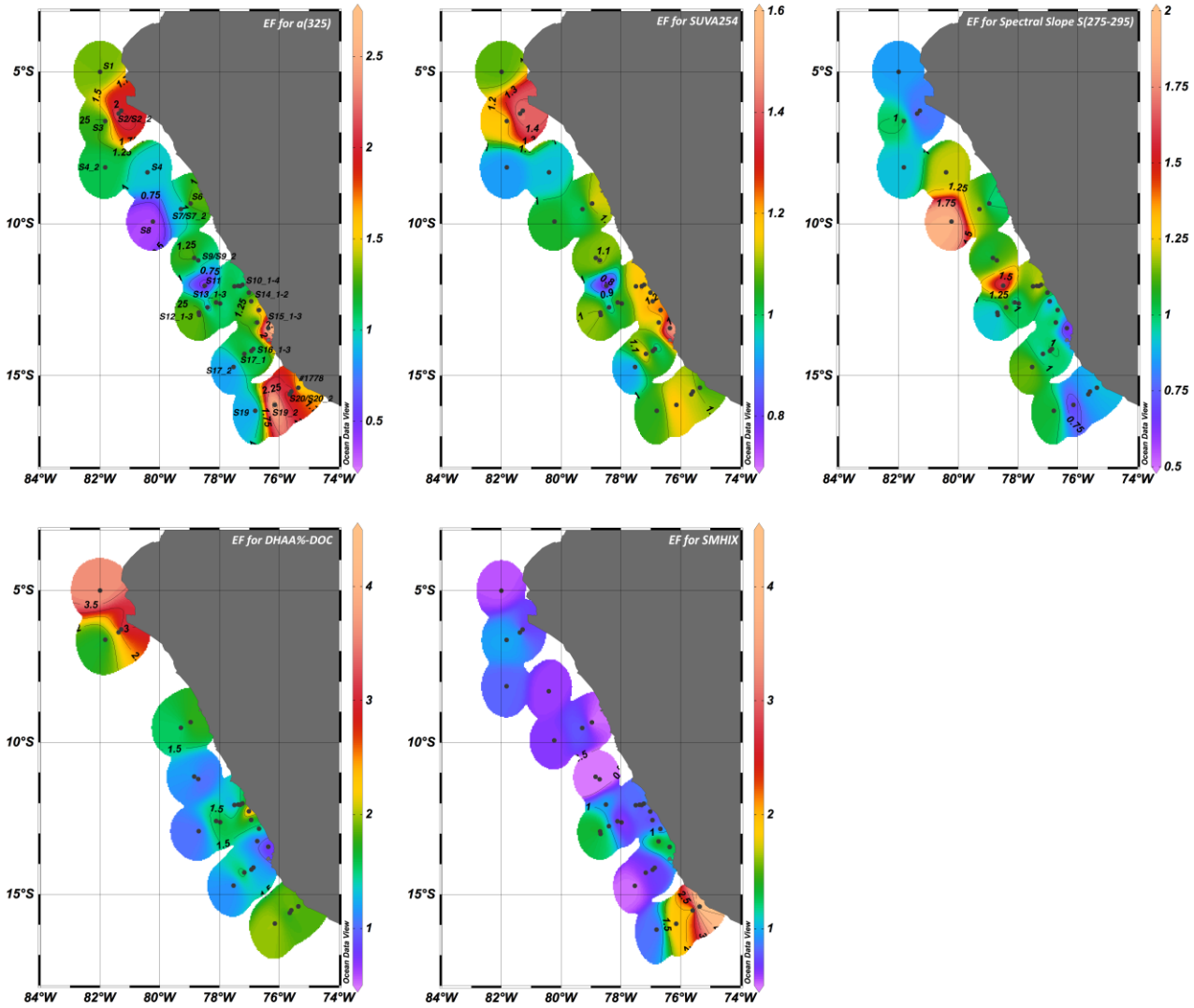
EF for a(325)
EF for SUVA254
EF for Spectral Slope S(275-295)
EF for DHAA%-DOC
EF for SMHIX
5°S
10°S
15°S
84°W
82°W
80°W
78°W
76°W
74°W
Ocean Data View

Figure 11

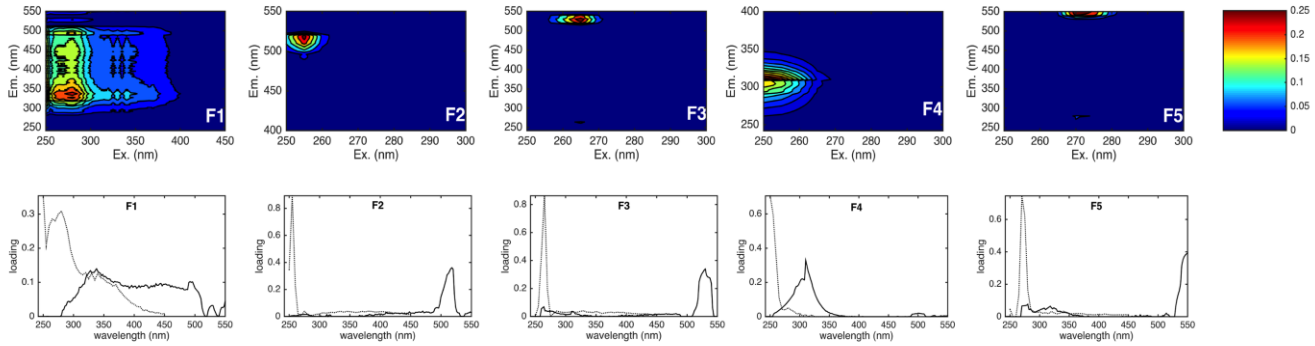

Figure 12

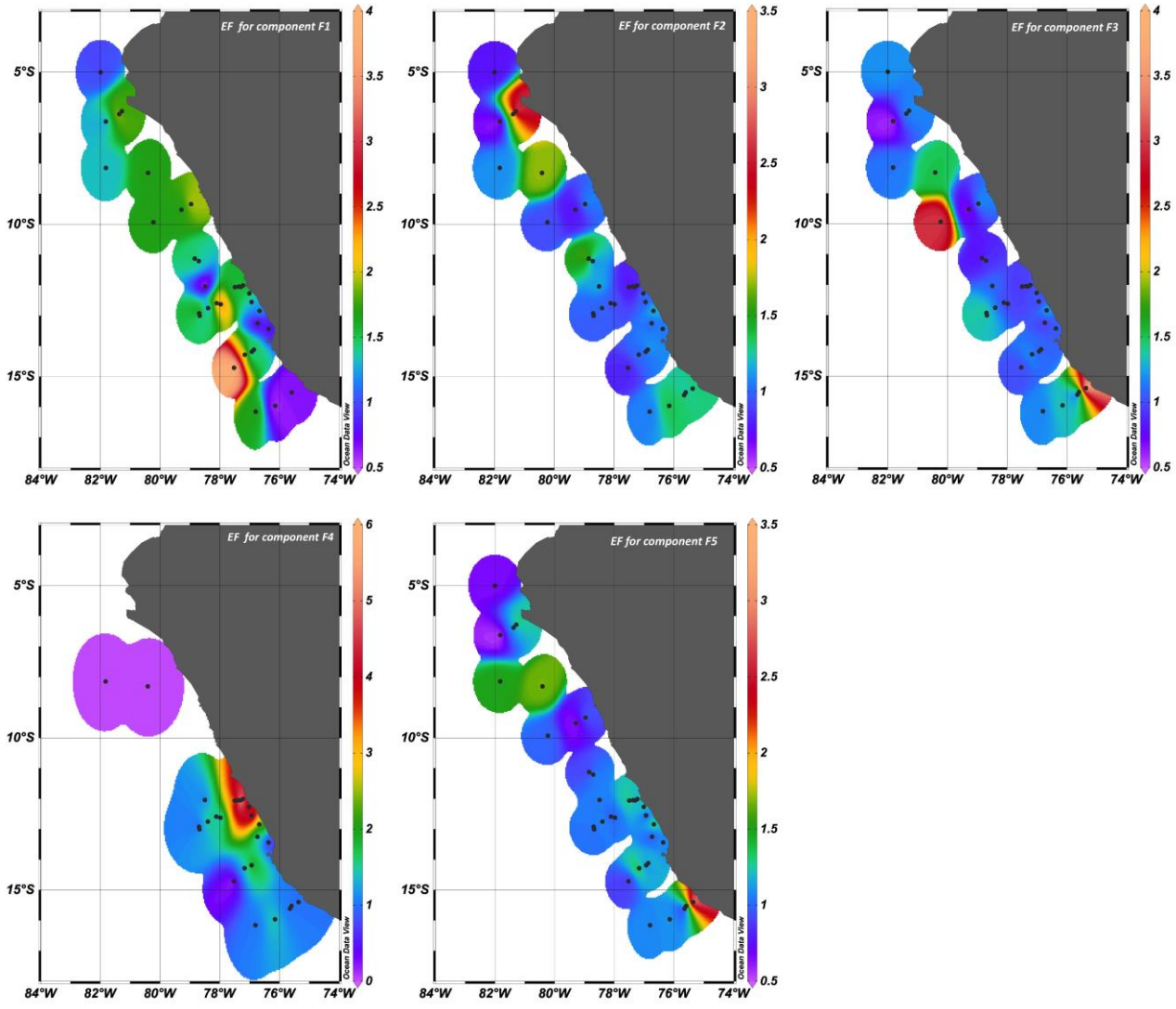

Figure 13

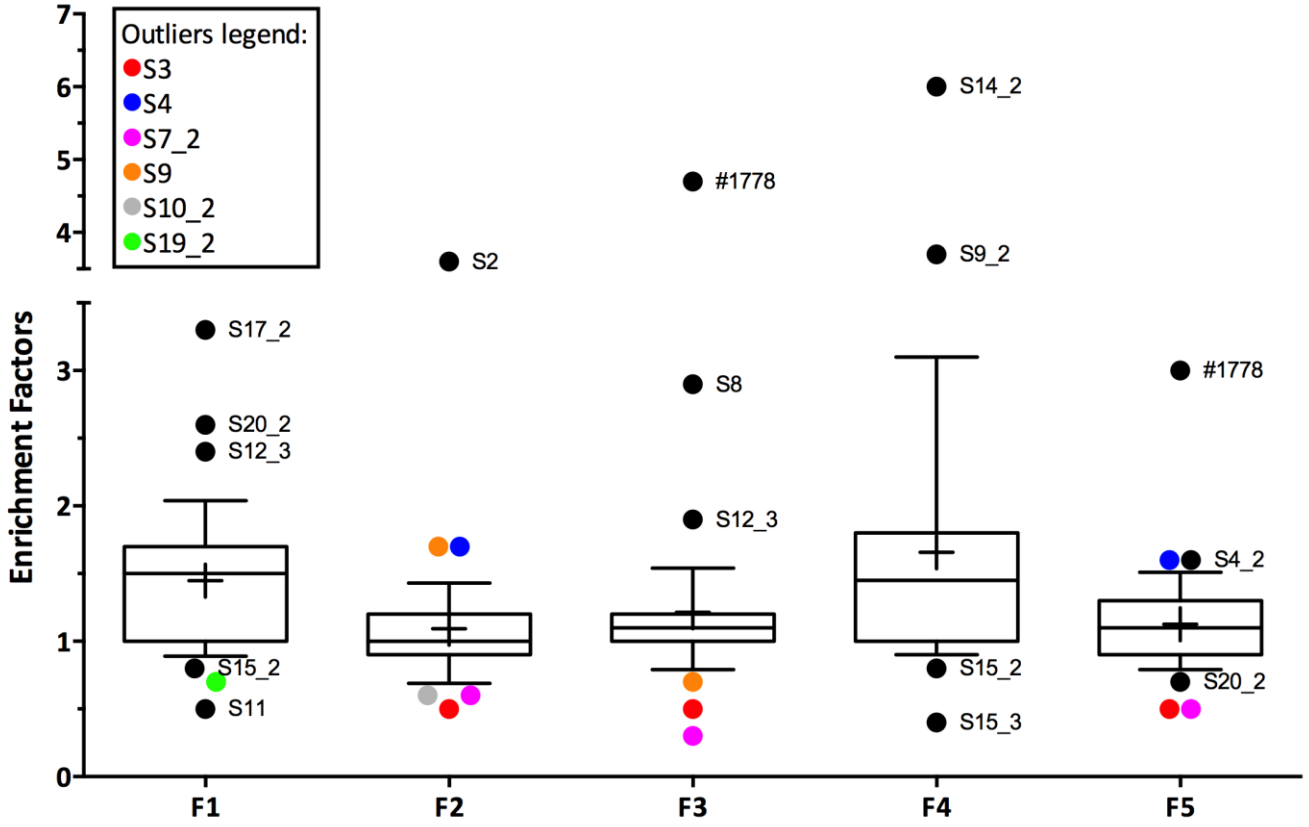
Outliers legend:
S3
S4
S7_2
S9
S10_2
S19_2
Enrichment Factors
7
6
5
4
3
2
1
0
S17_2
S20_2
S12_3
S15_2
S11
S2
#1778
S8
S12_3
S14_2
S9_2
S15_2
S15_3
#1778
S4_2
S20_2
F1
F2
F3
F4
F5

Figure 14

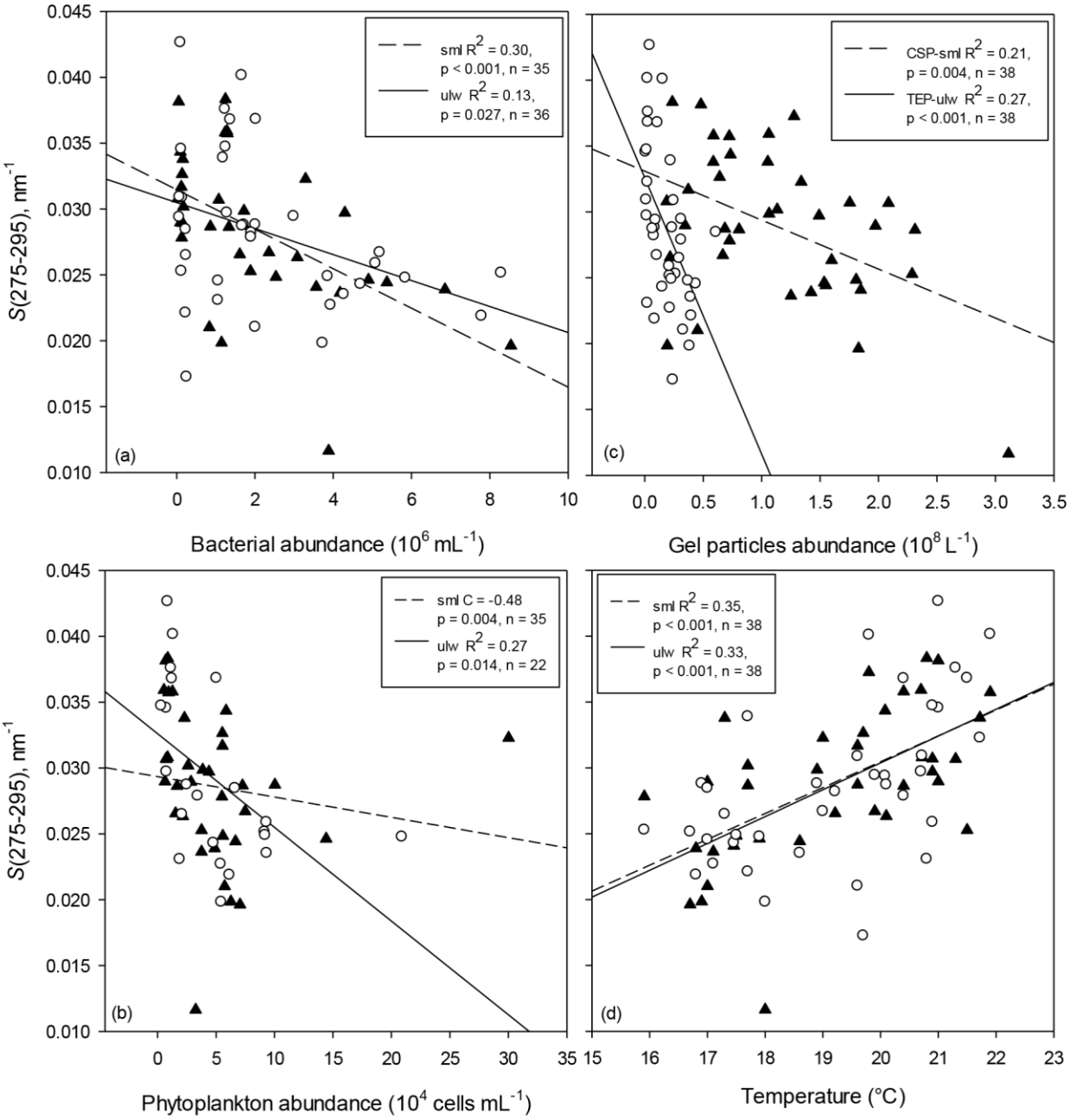
S(275-295), nm-1
sml R2 = 0.30,
p < 0.001, n = 35
ulw R2 = 0.13,
p = 0.027, n = 36
(a)
Bacterial abundance (10^6 mL^-1)
CSP-sml R2 = 0.21,
p = 0.004, n = 38
TEP-ulw R2 = 0.27,
p < 0.001, n = 38
(c)
Gel particles abundance (10^8 L^-1)
sml C = -0.48
p = 0.004, n = 35
ulw R2 = 0.27
p = 0.014, n = 22
(b)
Phytoplankton abundance (10^4 cells mL^-1)
sml R2 = 0.35,
p < 0.001, n = 38
ulw R2 = 0.33,
p < 0.001, n = 38
(d)
Temperature (°C)

Figure 15